UNIVERSITÀ DEGLI STUDI DI UDINE

Dipartimento di Scienze e Tecnologie Biomediche

Tesi di Dottorato
in
Scienze Biomediche e Biotecnologiche
XXVI CICLO

Role of p70S6K and STAT3 signaling pathways in breast cancer recurrence

RELATRICE
Dott. ssa Barbara Belletti

DOTTORANDA
Dr.ssa Ilenia Segatto

CORRELATORE
Dott. Gustavo Baldassarre

COORDINATORE
Prof. Claudio Brancolini

Anno Accademico 2013-2014

TABLE OF CONTENTS

ABSTRACT

For early breast cancer (EBC) patients, local relapse represents what mostly influences disease outcome. Surgery itself and the consequent process of wound healing have been proposed to stimulate local recurrences via pathway(s) still to be clarified. Notably, 90% of local recurrences occur at or close to the same quadrant of the primary cancer. p70S6K and STAT3 pathways have been implicated in breast cancer cell response to post-surgical inflammation, supporting the hypothesis that they may be crucial also for breast cancer recurrence. The results of this PhD thesis show that interfering with p70S6K activity strongly impaired breast cancer cell survival *in vitro* and local relapse *in vivo*. Peri-operative treatment using specific pharmacological inhibition of p70S6K1 was sufficient to reduce by 83% the rate of local recurrence. The significance of our results was confirmed in human EBC specimens, proving that p70S6K activity is consistently increased by surgery, also in human patients. Our study also highlighted that surgical fluids very efficiently activated STAT3 and that STAT3 activity was necessary for the survival and growth of tumor initiating cells. Taken together, our results show that p70S6K and STAT3 pathway are strongly involved in the promotion of the survival of residual tumor cells in the breast microenvironment.

Moreover, we demonstrate that p70S6K is an important regulator of breast cancer progression and could be used as target to restrain recurrent disease and to improve clinical outcomes in EBC patients. Finally, we show that STAT3 impinges on breast cancer stem cell phenotype upon WF stimulation and its precise role in the insurgence of local recurrence is currently under investigation.

1. INTRODUCTION

1.1 Breast Cancer

Breast cancer is the most frequently diagnosed cancer in women worldwide and the second leading cause of cancer-related death. More than 1-2 million cases are diagnosed every year, affecting 10–12% of the female population and accounting for 500,000 deaths per year worldwide (1). In the last two decades, mortality rates have generally remained stable or decreased. Declines in breast cancer mortality have been attributed to both novel treatment strategies and early detection due to the implementation of screening/prevention programs (2). However, more than 120,000 estimated deaths due to breast cancer are expected annually in the US and Europe combined (3, 4). Breast cancer is not a single disease: it is instead a collection of breast diseases that are heterogeneous in terms of histology, genetic and genomic variations, therapeutic response and patient outcomes. From a clinical point of view, breast cancer can be subdivided into three major subtypes: tumors expressing estrogen receptors (ERs) and/or progesterone receptors (PRs), tumors expressing amplified form of human epidermal receptor 2 (HER2-amplified) and tumors commonly referred to as triple-negative breast cancer (TNBC), due to lack of or low positivity for ER, PR and HER2 (5). These markers together with other clinical parameters (age, node status, tumor size, histological grade) are routinely used in the clinic to stratify patients for prognostic predictions and treatment selection. However, the complexity of breast cancer diseases is not entirely reflected by the parameters described. Studies based on global gene expression analyses have provided important new classifications of cancer patients based on variations in their gene expression profiles that correlated with prognosis (6-9). The studies of gene expression profiling reported by Perou et al. have established five breast cancer intrinsic subtypes (Luminal A, Luminal B, HER2-enriched, Claudin-low, Basal-like) and a Normal Breast-like group. Importantly, the intrinsic subtypes segregated tumors by expression of hormone receptors (both ERs and PRs), supporting earlier epidemiologic and biomarker studies. Among the ER-positive tumors, two major subtypes, luminal A and luminal B, have been identified. These subtypes are biologically distinct in that luminal A tumors tend to have higher expression of ER related genes and lower expression of proliferative genes than luminal B (6-9). Among the ER-negative tumors, the major subtypes are the HER2-enriched subtype and the basal-like subtype. The first group shows elevated expression of HER2 and of many other genes residing near HER2 in the genome. The basal-like subtype includes the triple-negative breast cancer and display high proliferative rate compared with other subtypes (6-9). Importantly, these subtypes have been shown to be clinically meaningful, and can

divide patients into groups with distinct tumor histotypes and distinct outcomes. Comprehensive characterization of molecular subtypes requires whole genome profiling which is not routinely performed in the clinical setting. For this reason, as mentioned before, the different classes of tumors are distinguished more easily by expression of the ER, PR, and HER2 receptors that are routinely performed to guide therapy decisions. For breast cancer patients, several treatment options are currently available in neoadjuvant or adjuvant settings. These include hormone therapies, targeted therapies, radiotherapy and various chemotherapy regimens. Breast cancer patients with positive ER, PR and HER2 status are responsive to targeted therapeutics given as monotherapy, or in combination with chemotherapy. A number of hormonal therapeutic agents have been approved for the treatment of ER positive disease, including tamoxifen, aromatase inhibitors and fulvestrant. For HER2 positive breast cancer, a growing number of HER2-targeted agents have become available, including trastuzumab, lapatinib and pertuzumab (5, 10).

1.2 Local Recurrence in Early Breast Cancer

The systemic use of widespread mammographic screening has contributed to a stage shift for newly diagnosed disease, increasing the percentage of early breast cancer (EBC) at diagnosis. In women with EBC all detectable cancer is restricted to the breast and, in women with node-positive disease, to the local lymph nodes. Breast conserving therapy, including primary tumor excision, axillary node dissection (determined in advance or decided following sentinel node sampling) and external radiotherapy (RT), is considered standard of care for management of women with early-stage breast cancer (11). For EBC patients the appearance of local relapse (LR, defined as the reappearance of malignant disease in the ipsilateral breast) represents a common event that may influence the prognosis. Several studies have shown that the presence of local recurrence is the strongest independent predictor of distant relapse and confers an increased risk of up to three-fold to four-fold (11, 12). Importantly, it was demonstrated that local recurrence formation is not merely associated with distant relapse but is causally related, indicating that local relapse is a determinant and not simply an indicator of risk of distant metastasis (13). The relapse of the disease in breast cancer occurs in one in five patients and represents the principal cause of breast cancer-related deaths (14). The relative risk of distant metastases for patients developing local relapse in comparison with patients without local relapse is considerable and, in fact, patients who develop LR present a substantially worse overall survival (15-17). The importance to restrain local recurrences in

breast patients was highlighted in a recent overview that conclusively showed that treatments substantially improving local control have definite effects on long-term survival, representing one life saved for every four loco-regional recurrences prevented (18).

The effects of external radiotherapy on local recurrence as well as on distant recurrence and long-term overall survival were recently extensively analyzed. A recent meta-analysis by the Early Breast Cancer Trialists' Collaborative Group (EBCTCG) has demonstrated that local radiation treatment to either the breast after breast-conservation surgery or the chest wall after mastectomy induced an overall survival benefit at 15 years (18). In particular, radiotherapy reduces the recurrence rate by half and the death rate by about a sixth in patients that have undergone breast conserving surgery. Results of the EBCTCG overview have reinforced the link between local control and mortality, emphasizing the importance of achieving the best loco-regional treatment for this kind of patients.

Interestingly, it was observed that a differential pattern of recurrence between different breast cancer subtypes exists (19-21). In particular, patients with luminal A (ER-positive) tumors had the most favorable prognosis, with LR of 8% at 10 years; conversely, TNBC patients exhibited a rate of 14% (22). Also the mean time to local relapse was shorter in patients with TNBC tumors than other breast cancer subtypes (23).

Clinical and experimental data suggest that the perturbation induced in the tumor microenvironment by surgery itself and the subsequent wound healing process may result in stimulation of postsurgical disease (24-26). From a clinical point of view, 90% of local recurrences occur at or close to the same quadrant of the primary cancer, despite multifocality is very common in breast cancer (27). Three-dimensional analysis of mastectomy specimens showed that 63% of breasts harbour occult cancer foci, with 80% of these situated remote from the index quadrant. However, the cancers in other quadrants of the breast appeared to remain dormant for many years and have a low risk of causing clinical tumors (27). Moreover, the results of a randomized clinical trial comparing mastectomy and quadrantectomy showed that early relapses were more frequent in the mastectomy than the quadrantectomy group. This difference, which disappeared later on during follow-up, is consistent with an acceleration of metastatic burden in the first years after invasive surgery (28). These clinical observations support the idea that local disease develops from re-growth of residual cancer cell in peritumoral tissue in response to surgical wounding. Experimental data in animal models, show that the surgical trauma enhances the proliferation of metastatic foci, supporting the hypothesis that, at least in mice, surgery should be considered as a major perturbing factor for metastasis (25). Some evidences highlighted that also in human breast

cancer, surgical removal of the primary tumor may induce changes in the growth kinetics of micro-metastasis, similarly to what observed in animal models (25). Indeed, many similarities between the stroma at sites of wound repair and reactive stroma in cancer can be observed, including inflammation, chemotaxis, angiogenesis and extracellular matrix production (29, 30). Since tumor progression requires continuous interactions between neoplastic cells and the microenvironment, a favorable wound healing stroma might promote the growth of residual cells into a tumor. The correlation between wound response and cancer progression was also supported by the analysis of gene expression profile of normal tissue adjacent to cancer that evidences the activation of a "wound response signature" able to promote cancer progression (31). The *in vivo* wound response signature is highly prognostic of breast cancer survival and suggests the idea that microenvironment represents an important variable for breast cancer progression, especially when a wound response is activated by surgical excision (31). Other studies performed in mice have shown the presence of growth stimulating factors in mouse serum after removal of the primary tumor (32). Recently, our (33) and other (34) *in vitro* studies demonstrated the stimulatory effect of post-surgical drainage fluids (hereafter referred to as wound fluids, WF) on breast cancer cells proliferation and invasion. Work from other groups reported that WF, as well as postsurgical serum samples, induce proliferation of HER2-positive breast carcinomas, signifying that at the site of surgery growth factors able to induce cell proliferation are produced (34). In our work, we found that WF collected from early breast cancer patients undergone to breast surgery, stimulated cancer cells growth, migration and invasion (33), supporting the role of surgery as perturbing factor for recurrence formation, also in human patients. Moreover, we evaluated whether treatment with intra-operative radiotherapy, such as TARGIT (Targeted Intraoperative RadioTherapy), may reduce local recurrence by killing residual tumor cells and also by affecting tumor microenvironment (33). TARGIT-A trial was launched on 2000 to test whether intraoperative radiotherapy might be considered an alternative to external radiotherapy (27, 35). Intraoperative radiotherapy delivers a high dose of radiation as one fraction at the time of surgery, allowing precise application of radiation dose to the target area around the surgical bed. The clinical relevance of one single application of TARGIT was recently reported, demonstrating that intraoperative treatments are much more effective than previously hypothesized (35). Our previous results (33) and clinical observations (35) suggest that this could be due, at least in part, to the alteration of the microenvironment and to the modulation of the wound healing response induced by intra-operative radiotherapy. In fact, our data clearly demonstrated that WF derived from TARGIT-treated patients were defective in stimulating breast cancer cell

proliferation and invasion, compared with WF from patients treated only with surgery (33). Moreover, we highlighted the importance of two pathways in this response, the p70S6K and the STAT3 pathway. The activation of these pathways is high when breast cancer cells are stimulated with surgical fluids but is impaired in the presence of WF derived from TARGIT-treated patients (33). For this reason, and given the clinical benefit observed in TARGIT–treated patients, we hypothesized that p70S6K and STAT3 could represent two key regulators in the mechanisms of local relapse in EBC patients.

1.3 p70S6K signaling and breast cancer

The PI3K/mTOR/p70S6K axis is known to regulate many processes that are critical for tumorigenesis such as cell growth, proliferation, survival and metabolism (36). Briefly, the activation of PI3K (phosphatidylinositol 3-kinase) and the production of the lipid second messenger PIP3 (phosphatidylinositol 3,4,5-trisphosphate) from PIP2 triggers the recruitment and activation of Akt (protein kinase B) by the phosphatidylinositol-dependent kinases, PDK1 and PDK2 (37). One of the major effectors downstream of Akt is mTOR. Akt phosphorylates and inactivates the tuberous sclerosis complex (TSC) tumor suppressor, leading to the activation of the mammalian target of rapamycin complex 1 (mTORC1, hereafter mTOR) signaling pathway that results in the activation of p70S6K (38) (Figure 1).

The described pathway is inappropriately activated in many cancers by receptor tyrosine kinases, as well as by the genetic mutation and amplification of other key pathway components. The aberrant activation of this pathway plays a major role in breast cancer and many evidences suggest that it is linked to promotion of breast cancer cell survival, resistance to chemotherapy, resistance to endocrine therapy, and it is associated with poor prognosis, advanced stage and histological grade (39-41).

mTOR is a conserved central regulator of cell proliferation and growth and integrates signals from multiple inputs such as growth factors, stress, nutrients, and energy to regulate protein synthesis, cell cycle progression, actin organization, and autophagy (42, 43). Because of these essential roles, deregulation of mTOR is prominent in the development and progression of cancer and in metabolic diseases, such as diabetes and obesity. Two families of mTOR substrates have been characterized: the ribosomal protein S6 kinases (S6K1–2), and the eIF4E-binding proteins (4EBP1–3). 4E-BP1 is a repressor of the translation initiation factor eIF4E and thus an inhibitor or protein biosynthesis; the phosphorylation triggered by mTOR

disrupts its interaction with eIF4E allowing eIF4E to bind and form a functional initiation complex (Figure 1).

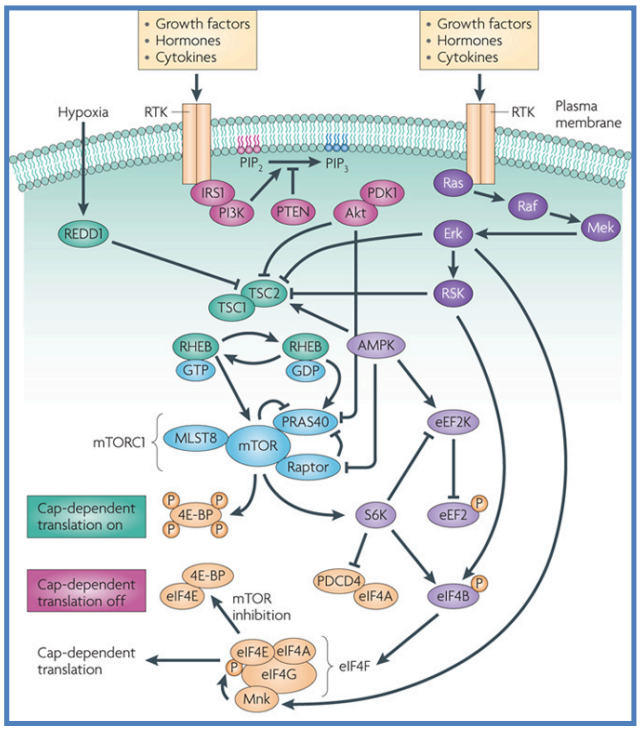

Figure 1. Schematic representation of PI3K/mTOR/p70S6K pathway. Mitogenic signals (growth factors, cytokines and hormones) act on receptor tyrosine kinases (RTKs), stimulating PI3K that in turn stimulates the Akt pathway. Akt activates mTORC1 which phosphorylates and activates ribosomal S6 kinases (S6Ks) (*adapted from Silvera et al., 2010*).

Opposite to 4E-BP1, S6K phosphorylation results in its activation and in initiation of the translation machinery through activation of several regulators of protein synthesis (42-46).

The ribosomal protein S6 kinase family comprises two homologous proteins, S6K1 and S6K2, each of which are found as two alternatively spliced isoforms (p70S6K and p85S6K). Both S6K1 and S6K2 are downstream of mTOR pathway and present same redundant functions. The p70 kDa isoform of S6K1 (p70S6K1) is the best-studied S6 kinase, it is ubiquitously expressed and localizes predominantly to the cytoplasm (47).

S6K1 belongs to the AGC kinase family, a subgroup of serine/threonine protein kinases. AGC kinases activation is dependent on the phosphorylation of two regulatory motifs: an activation loop and a hydrophobic motif (37). For S6K1, the best characterized sites are Threonine 229 (T229) in the activation loop and Threonine 389 (T389) in the hydrophobic motif. mTOR

phosphorylates T389, relaxing the conformation of the kinase and creating a docking site for PDK1, which is then able to phosphorylate T229 in the activation loop (48).

S6K1 plays important roles in cell growth, proliferation, and cell differentiation by regulating protein synthesis, cell cycle progression, and metabolism (49-51). The principal substrate of the S6Ks is the ribosomal protein S6, one of 30 distinct ribosomal proteins, which together with 18S rRNA, constitutes the smaller 40S ribosomal subunit (52). The phosphorylation of S6 is a highly conserved event and occurs in five serine residues proceeding in a sequential fashion: S235-S236-S240-S244-S247. p70S6Ks are able to carry out the phosphorylation of all five sites (53, 54).

The physiological role of S6K was studied through genetic studies in Drosophila and mice. S6K-/- flies and mice are much smaller than wild type and this reduction in body size is due to a reduction in individual cell size rather than cell number, suggesting that S6K mostly regulates cell growth rather than proliferation (51, 55, 56). However, in S6K1 knock-out mice S6K2 expression is upregulated and appears able to restore phosphorylation of S6 to levels close to those of wild type mice in all tissue examined, suggesting that S6K2 can cooperate and also substitute S6K1 in the phosphorylation of S6 (56, 57). Other targets of p70S6K have been reported, some of which include other regulators of protein synthesis such as the eukaryotic elongation factor 2 kinase (eEF2K), the eukaryotic translation initiation factor 4B (eIF4B), the translational inhibitor PDCD4 and the RNA-binding protein SKAR (58-61). S6K1 is able to phosphorylate also mTOR at Threonine 2446/Serine 2448, indicating that a potential feedback loop may exist (62) (Figure 2).

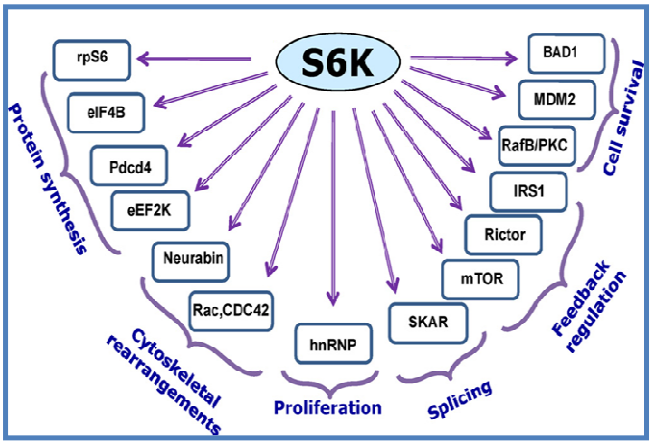

Figure 2. Key downstream effectors of S6K signaling. The image show the S6K downstream substrates and the cellular function in which are implicated (*adapted from Fenton and Gout, 2010*).

The complexity is increased by the fact that, although mTOR is known to be the primary regulator of S6K, other upstream activators of p70S6K were identified. For example, it was recently demonstrated that GSK-3 positively regulates S6K1 activity and cell proliferation, suggesting also that the cooperation of other upstream molecules is important for full activation and functionality of S6K (50).

In many cancers, the mTOR/S6K pathway is highly active because of mutations and/or overexpression of upstream positive regulators such as PI3K, Akt, and HER2, or loss of expression or function of negative regulators such as the tumor suppressors PTEN and TSC1/2. Recent studies have addressed the specific role of S6K1 in tumor proliferation, invasiveness, motility and angiogenesis (63, 64). In particular, many data suggest the involvement of p70S6K also in breast cancer onset and/or progression. p70S6K1 is encoded by the RPS6KB1 gene, localized to the chromosomal region 17q23. Comprehensive analysis of the 17q23 region revealed a limited number of highly expressed genes that may contribute to the more aggressive clinical course observed in breast cancer patients with 17q23-amplified tumors. It was observed that RPS6KB1 was amplified in 59 (8.8%) of 668 primary breast tumors and in several breast cancer cell lines, leading to the overexpression of the protein (65-68). It is to note that, while amplification of this region has been observed in several tumor types, high copy number amplification occurs in breast cancer specifically (68). Further evidence in support of a role for p70S6K1 in tumor development and progression comes from the observation that RPS6KB1 amplification and overexpression are associated with poor prognosis in an unselected series of breast cancer patients (67). Interestingly, in a study exploring the phosphorylation and activation of different members of the PI3K/Akt/mTOR pathway, phosphorylation of p70S6K (in T389 residue) has been found elevated 10- to 35-fold in breast cancer cells compared to normal primary mammary epithelial cells (69). Moreover, more than 70% of invasive breast carcinomas, have been demonstrated to possess high levels of phosphorylated p70S6K and, in sharp contrast, phosphorylation of the same protein was nearly undetectable or was at low levels in normal mammary tissues under the same assay (69).

Interestingly, overexpression of p70S6K protein is linked to increased risk of locoregional recurrence in node-negative EBC patients, thus specifically suggesting a role for this kinase as prognostic marker (70). Since frequent deregulation in the PI3K/AKT/mTOR/p70S6K signaling pathway was observed in different type of tumors, many efforts have been employed to develop several inhibitors at different levels of this pathway (5, 36). Among others, mTOR inhibitors are the most highly developed of this pathway. The first mTOR

inhibitor discovered was rapamycin, which is a macrolide that was originally found as an antifungal agent and was later recognized as having immunosuppressive and anticancer properties (71, 72). The mechanism of action of rapamycin is not completely understood. The complex of rapamycin with its intracellular receptor FKBP12 binds directly to mTORC1 and suppresses mTORC1-mediated phosphorylation of the substrates. Many rapamycin derivates were developed explicitly designed for development as anti-cancer drug (71). Despite the substantial pre-clinical data indicating that rapamycin and its analogues have anti-tumor effects and that mTOR participates in many cancer-related pathways, these molecules have not shown universal anti-tumor activity in early clinical trials. There are many reports of rapamycin promoting pro-apoptotic stimuli (73, 74) but there are also reports of it promoting cell survival (75, 76). It has been shown in breast tumors and in many cancer cell lines that inhibition of mTOR with rapalogs releases a negative feedback loop, resulting in re-activation of AKT. Despite the many strong correlative clinical and experimental observations, the role of p70S6K in the process of breast cancer relapse has never been investigated nor p70S6K has been exploited as a therapeutic target.

1.4 STAT3 signaling and breast cancer

Inflammatory conditions can initiate or promote oncogenic transformation and cancer associated inflammation is marked by the presence of specific inflammatory cells and inflammatory mediators, including cytokines and chemokines (77). Recent evidences suggest a crucial role for Signal Transducer and Activator of Transcription (STAT) family proteins, especially STAT3, in selectively inducing and maintaining a pro-carcinogenic inflammatory microenvironment, both at the initiation of malignant transformation and during cancer progression (78, 79). STAT3 belongs to the STAT family of proteins, which are both signal transducers and transcription factors. At least seven members in this family have been identified, which are encoded by distinct genes. Structurally, STAT proteins have the following distinct domains: the N-terminal, coiled-coil, DNA binding, the Linker, Src homology 2 (SH2) and C-terminal transactivation domains. Each of these domains has a distinct function. For example, the N-terminal domain is important in STAT dimer-dimer interactions; the DNA binding domain forms complexes between STAT proteins and DNA; the SH2 domain engages in dimerization between two activated STAT monomers through reciprocal phospho-tyrosine (pTyr)-SH2 domain interactions, while the C-terminal portion of the protein functions as the transcriptional activation domain (79-81). STAT3 has important

roles in fundamental processes, including proliferation, development, differentiation, inflammation, and apoptosis (79-82). STAT3 is activated by non-receptor tyrosine kinases, such as JAK or Src and growth factor receptor, such as epidermal growth factor receptor (EGFR) and platelet-derived growth factor receptor (PDGFR) (83, 84). Upon the binding of growth factors or cytokines to their cognate receptors on the cell surface, STAT3 is recruited to the cytoplasmic portions of the receptors, where it becomes phosphorylated on Tyr 705 in the C-terminus. Cytokine receptors do not usually have intrinsic tyrosine kinase activity: instead, their engagement activates receptor-associated tyrosine kinases, most prominently the Janus kinase (JAK) family kinases that are able to phosphorylate STAT3. Tyrosine-phosphorylated STAT3 then dimerizes through reciprocal pTyr-SH2 domain interactions, translocates into the nucleus and binds to specific STAT-response elements in the promoters of target genes, thereby inducing the transcription of those genes essential for its physiological functions (85-88) (Figure 3).

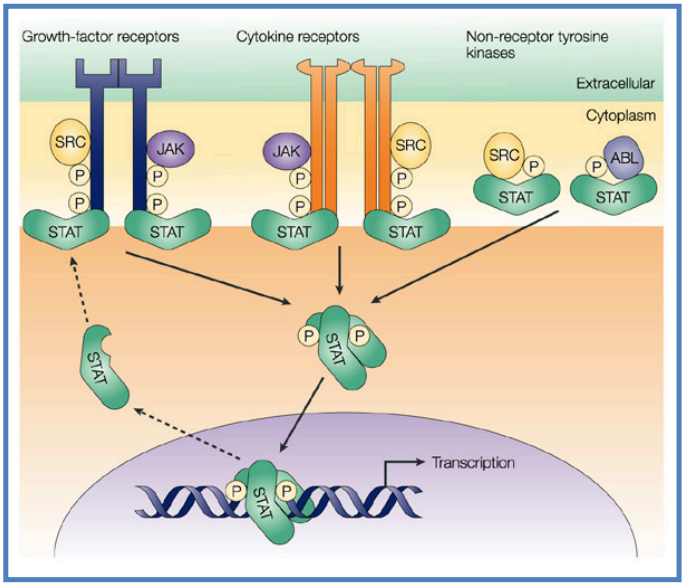

Figure 3. Schematic representation of STAT3 pathway. Binding of growth factors or cytokines to their receptors results in the activation of intrinsic receptor-tyrosine-kinase activity or of receptor-associated kinases, such as the JAK or Src tyrosine kinases. These tyrosine kinases subsequently phosphorylate the cytoplasmic tails of the receptor to provide docking sites for the recruitment of monomeric STAT3. Once they have been recruited, STAT3 becomes substrates for tyrosine phosphorylation. Phosphorylated STAT3 dimerizes and translocates to the nucleus, where the dimers directly regulate gene expression (*adapted from Yu and Jove, 2004*).

STAT3 regulates the transcription of several genes, some involved in apoptosis, such as Bcl-2, Bcl-xl, Mcl-1 and Survivin, others involved in cell cycle progression, such as Cyclin D1 and others related to epithelial-mesenchimal transition, such as Twist1 and Vimentin (78-82) (Figure 4). It is to note that many of the downstream target genes of STAT3 encode cytokines and growth factors, the receptors of which signal through the same STAT3, thereby providing a mechanism for autocrine and paracrine STAT3 activation (85, 88-90). Under normal biological conditions, STAT3 activation is rapid and transient. However, STAT3 has been found to be hyper-phosphorylated and constitutively activated in a large number of solid tumors and in cell lines which often become addicted to its activity for continuous survival and growth (91, 92).

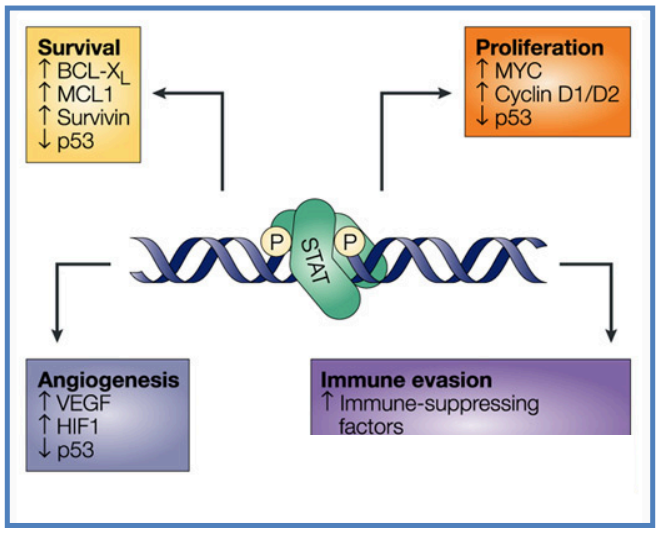

Figure 4. STAT3 target genes. STAT3 upregulates the expression of genes that are required for proliferation and survival. These include the genes that encode c-MYC, cyclin D1 and cyclin D2, BCL-xl, MCL1 and Survivin. In addition, STAT3 negatively regulates the expression of p53. STAT3 signaling also stimulates tumor angiogenesis (*adapted from Yu and Jove, 2004*).

The role of STAT3 in promoting transformation is well documented. Conditional knockout of the STAT3 gene or inhibition of STAT3 function blocked v-Src induced transformation in cancer model systems (93-95), indicating a pivotal role for STAT3 in malignant transformation. As an important proof for the oncogenic potential of STAT3, an artificially engineered, constitutively dimerized STAT3C alone is sufficient to induce malignant transformation of immortalized fibroblasts and tumor formation in mice (96). Gene

expression changes induced by constitutively active STAT3 represent critical molecular events that lead to the dysregulation of cell cycle control and apoptosis, thereby promoting cell growth and survival and contributing to malignant transformation and tumorigenesis. Despite many known pro-proliferative or anti-apoptotic target genes have been identified upon acute stimulation, they are not always consistently induced in tumors displaying lower but continuous STAT3 phosphorylation. The exact mechanisms by which constitutively active STAT3 mediates malignant transformation and human tumor formation are still incompletely understood and continue to be investigated.

Constitutive activity of STAT3 was observed in 35% to 60% of human breast tumors and in many breast cancer cell lines in which is required for continuous proliferation and resistance to apoptosis. Since no STAT3 mutation was identified, constitutive activation of STAT3 in breast tumors is associated with the induction of the expression and/or the activity of the EGF receptor family kinases and of Src or also with aberrant JAK activity (97-101). Several studies have used different approaches to assess the expression, localization, phosphorylation, and DNA binding ability of STAT3 in breast cancer. One of these studies has found increased levels of nuclear localized STAT3 in comparison to normal surrounding tissues but no association with clinico-pathological or outcomes data were provided (102). Another study assessed the level of STAT3 and phospho-STAT3 in several samples of node-negative breast cancer patients and correlated these results with clinico-pathological and survival data (103). This study found that nuclear phospho-STAT3 expression was correlated with a modest, but statistically significant, improvement in patient survival both at 5 and 20 years. Data from *in vitro* studies have evidenced that pharmacological or dominant-negative inhibition of STAT3 activity has been found to block the proliferation and survival of breast cancer cells in part by down-regulation of Bcl-xL, Bcl-2, Survivin and Mcl-1, and correlated well with the inhibition of human breast tumor growth in xenograft models (98, 100, 104, 105). However, little data exists regarding STAT3 -mediated gene up-regulation in malignant breast tissues and the specific contributions of the genes regulated by STAT3 during the pathogenesis of human breast cancer remain to be completely elucidated.

Recently, some authors have reported the involvement of cytokine signaling via IL6 receptor/STAT3 in the regulation of breast cancer stem cells (CSCs) self renewal and differentiation (106, 107, 110-113). Cancer stem cells or tumor initiating cells (TICs) are rare cells that are suspected to be responsible for tumor recurrence, formation of metastases, as well as chemoresistance (108, 109). It was demonstrated that activated JAK2/STAT3 signaling is essential for the survival of CD44+/CD24-/low stem-like breast cancer cells (110)

and was shown to play an important role during mammosphere formation (111). STAT3 was also identified by a RNAi screen to be a critical player in mammosphere formation and self renewal of breast CSCs (112, 113). Despite the fact that a sizable body of evidences highlight that STAT3 is inappropriately activated in a vast percentage of breast tumors, its biological significance is not fully established and its concrete role in breast cancer initiation and/or progression is still very controversial.

Since the discovery of the association of constitutive STAT3 activation with malignant transformation, a large number of studies have been undertaken for the validation of STAT3 as a cancer drug target (114-116), and substantial efforts were employed into the discovery of novel STAT3 inhibitors. There is a large number of STAT3 inhibitors reported, with many different mechanism of actions. Of these inhibitors, a few show good activity in terms of the inhibition of STAT3 biological functions and the associated antitumor cell effects, as well as the inhibition of tumor growth in the mouse models of human tumors (116). These inhibitors are mostly at the experimental stage and not in the form considered to be suitable for clinical utility; in fact, up to now, only two drugs are in the first phase of clinical trial.

2. AIMS

Breast cancer represents the most common malignancy in women worldwide. Local relapse represents what mostly influences the outcome in early breast cancer patients (EBC). Thus, the understanding of the mechanisms underlying this unfavorable clinical event represents a compelling objective in breast cancer research. Despite the fact that multifocality is a hallmark of most breast cancer, 90% of local recurrences occur at the same quadrant of the primary cancer, supporting the hypothesis that surgery itself and the consequent process of wound healing may represent a perturbing factor in the mechanism that lead to local re-growth. Our previous work evidenced p70S6K and STAT3 signaling pathway as possible molecular mediators of breast cancer recurrence. In this PhD project, we aimed to dissect the role of p70S6K and STAT3 signaling pathways in the response of breast cancer cells to wound fluids and to understand their possible contribution in regulating the processes that provokes the insurgence of local recurrences.

To this aim, we characterized the behavior of breast cancer cell lines with impaired p70S6K or STAT3 activity with particular interest to WF response. As additional approach, we used a novel specific pharmacological inhibitor of p70S6K1 and different compounds targeting STAT3.

We designed an *in vivo* experimental model resembling the course of human breast cancer, in which breast cancer cells were injected in nude mice mammary fat pads and, when primary tumors were grown, masses were surgically removed under anesthesia. After recovering, mice were followed up to detect appearance of local relapse.

Using this model, we dissected the role of p70S6K and STAT3 during breast cancer growth and recurrence by modulating their activity using both genetic and pharmacologic approaches. Our results show that p70S6K and STAT3 pathways positively affect the survival of residual breast cancer cells. We demonstrated that p70S6K is an important regulator during the process of breast cancer recurrence and could be used as target to restrain recurrent disease and to improve clinical outcomes in EBC patients. Moreover, we show that STAT3 impinges on breast cancer stem cell phenotype upon WF stimulation and its precise role in the insurgence of local recurrences is under evaluation.

3. RESULTS

3.1. Role of p70S6K signaling pathway in breast cancer recurrence

3.1.1. Generation of breast cancer cell lines with altered p70S6K activity.

Our previous studies demonstrated that wound fluids (WF) collected from the breast wound after surgery of EBC patients are very rich in cytokines and growth factors, stimulated breast cancer cell proliferation, motility and invasion, and induced a marked activation of the p70S6K pathway (33). Using a larger panel of breast cancer cell lines, we confirmed that activation of p70S6K signaling is a common event after exposure to WF (Figure 1A-B). The analysis of the p70S6K target phospho-S6 showed that, with few exceptions, 5% WF stimulated p70S6K signaling at even higher extent than 10% serum.

To investigate whether activation of p70S6K was functionally involved in the response of breast cancer cells to WF, we generated breast cancer cell lines with altered p70S6K activity (Figure 2A-B and data not shown). We chose to use two triple negative carcinoma cell lines with highly aggressive phenotype, MDA-MB-231 and MDA-MB-453. To this aim, cells were transfected with a kinase inactive form of p70S6K (HA-p70KR, carrying the substitution K100R) (117) (Figure 2A) or transduced with lentiviral particles encoding for specific anti human p70S6K sh-RNA (Figure 2B). As additional approach, we also used a novel specific p70S6K1 inhibitor, PF-4708671 (hereafter PF) (118), as well as the clinically approved mTOR inhibitor, rapamycin analogue Temsirolimus (hereafter Tems). Cells were then stimulated with FBS or WF and activation of p70S6K evaluated (Figure 2A-C and data not shown).

Our experiments clearly indicated that breast cancer cells responded to WF stimulation hyper-activating p70S6K pathway and this activation was efficiently impaired when p70S6K pathway was blocked by different approaches.

3.1.2. Characterization of proliferative and migratory behavior of breast cancer cell lines with altered p70S6K activity.

We then analyzed the effects of alteration of p70S6K activity in proliferative and migratory behavior of cells. Since WF are rich in cytokines and growth factor, we used either WF or FBS as source of growth stimuli. In line with the well established role of p70S6K in cell proliferation, growth curve assay revealed that, when p70S6K activity was impaired, moderate but consistent decrease of cell proliferation was always observed (Figure 3A-B and data not shown). Consistently, growth of the parental cells in the continuous presence of PF or Tem led to a similar reduction of proliferation rate (Figure 3B). More importantly, using

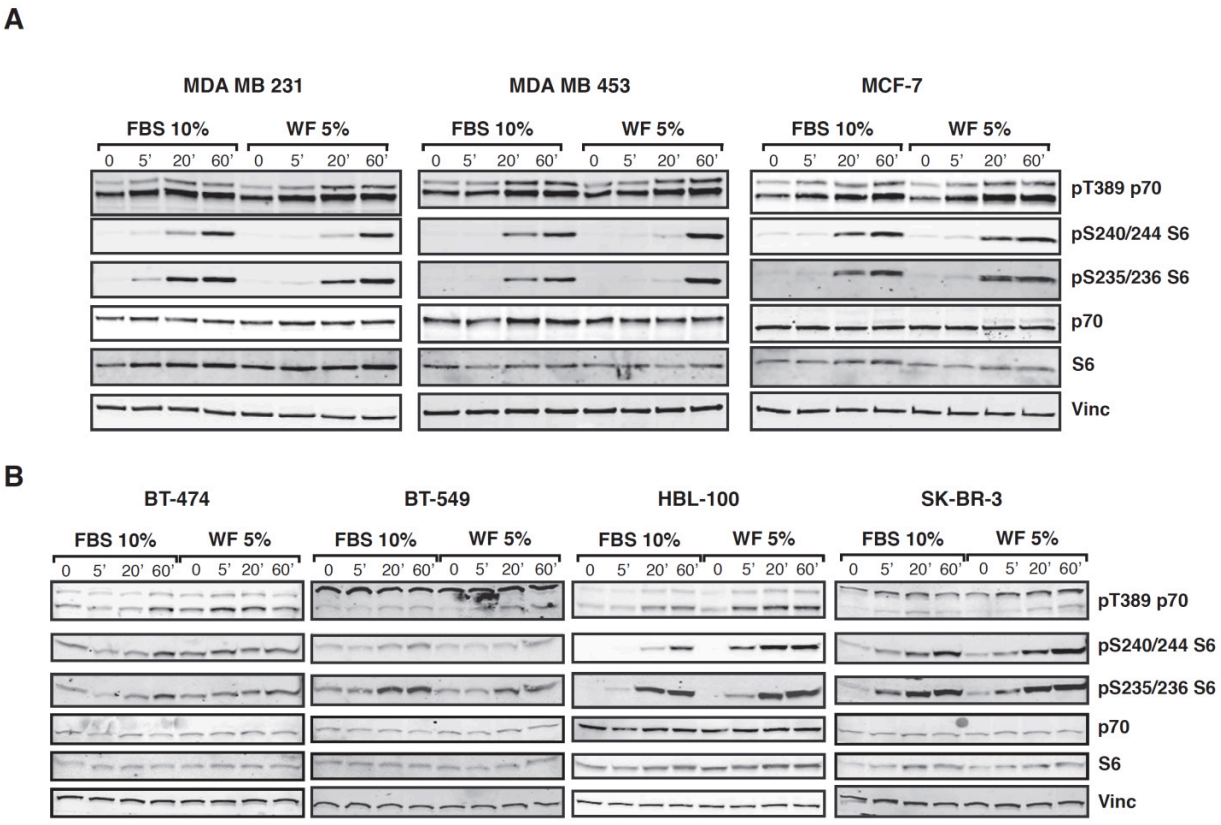
A
MDA MB 231
MDA MB 453
MCF-7
FBS 10%
WF 5%
0 5' 20' 60'
pT389 p70
pS240/244 S6
pS235/236 S6
p70
S6
Vinc
B
BT-474
BT-549
HBL-100
SK-BR-3
FBS 10%
WF 5%
0 5' 20' 60'
pT389 p70
pS240/244 S6
pS235/236 S6
p70
S6
Vinc

Figure 1. In breast cancer cell lines, p70S6K is efficiently activated following stimulation with wound fluids.

A. Western blot analysis of MDA-MB-231, MDA-MB-453 and MCF-7 cell lines serum starved and then stimulated for the indicated times with 10% serum (FBS) or 5% wound fluids (WF). **B**. Same as in (A), but using BT-474, BT-549, HBL-100 and SK-BR-3 cell lines, as indicated. Vinculin expression was used as loading control.

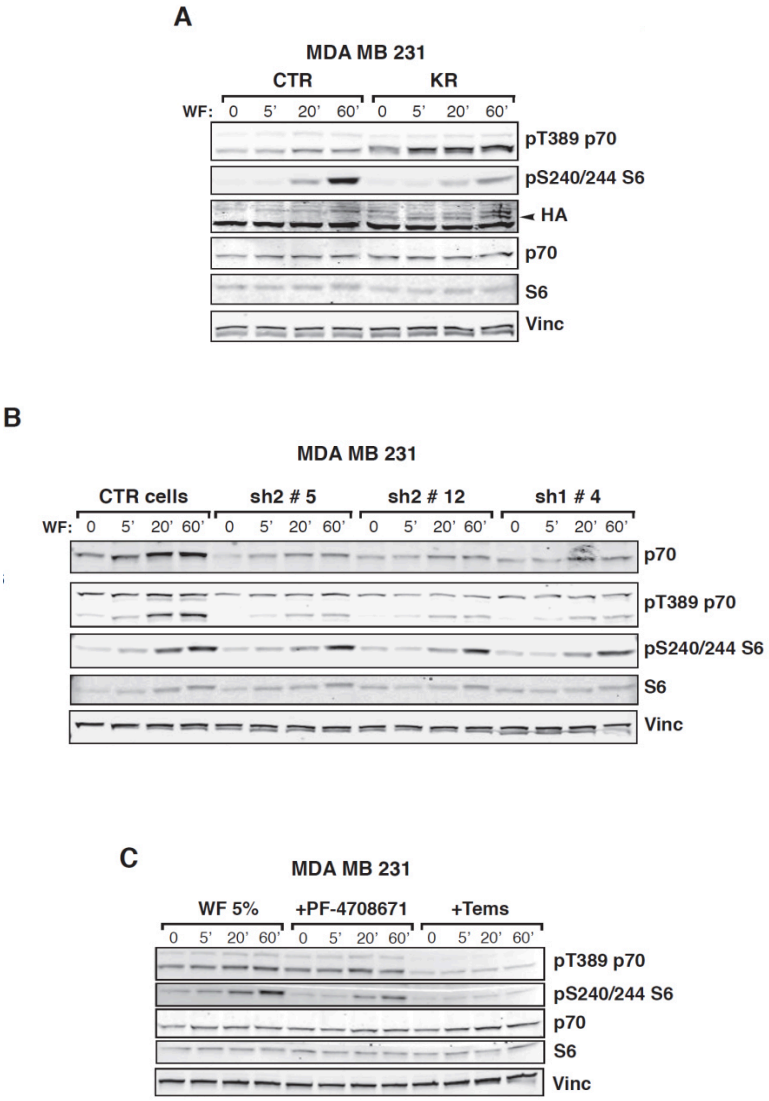
A
MDA MB 231
CTR
KR
WF: 0 5' 20' 60' 0 5' 20' 60'
pT389 p70
pS240/244 S6
HA
p70
S6
Vinc
B
MDA MB 231
CTR cells
sh2 # 5
sh2 # 12
sh1 # 4
WF: 0 5' 20' 60' 0 5' 20' 60' 0 5' 20' 60' 0 5' 20' 60'
p70
pT389 p70
pS240/244 S6
S6
Vinc
C
MDA MB 231
WF 5%
+PF-4708671
+Tems
0 5' 20' 60' 0 5' 20' 60' 0 5' 20' 60'
pT389 p70
pS240/244 S6
p70
S6
Vinc

Figure 2. Activation of p70S6K following wound fluid (WF) stimulation is efficiently impaired in breast cancer cell lines modified for p70S6K expression or inhibited for its activity. A. Western blot analysis of MDA-MB-231 cell line stably transduced with a retroviral empty vector (CTR) or with a retroviral vector encoding for a kinase inactive mutant of p70S6K (KR), serum starved and then stimulated for the indicated times with wound fluids (WF).**B.** Western blot analysis of MDA-MB-231 cell line stably transduced with a lentiviral vector encoding for control sh-RNA (CTR) or for sh-RNAs directed against human p70S6K (sh), serum starved and then stimulated for the indicated times with wound fluids (WF).**C.** Western blot analysis of MDA-MB-231 cell line serum starved and then stimulated for the indicated times with wound fluids (WF) or serum starved, pre-treated 30 minutes with the indicated inhibitor (PF-4708671 10 μM or Temsirolimus 100 nM) and then stimulated for the indicated times with WF, in the presence of the inhibitor. Vinculin expression was used as loading control.

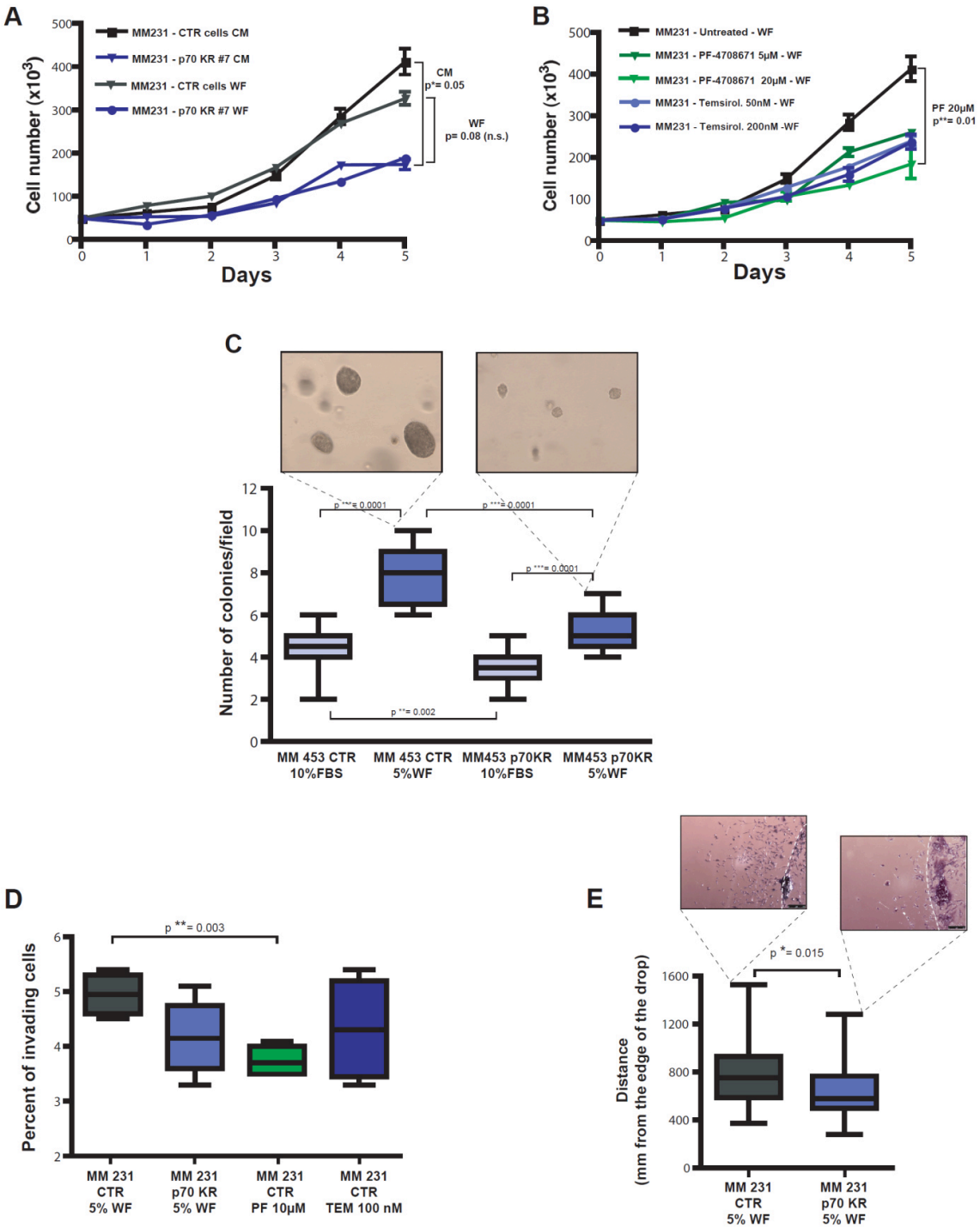
A
MM231 - CTR cells CM
MM231 - p70 KR #7 CM
MM231 - CTR cells WF
MM231 - p70 KR #7 WF
Cell number (x10³)
Days
CM
p*= 0.05
WF
p= 0.08 (n.s.)
B
MM231 - Untreated - WF
MM231 - PF-4708671 5μM - WF
MM231 - PF-4708671 20μM - WF
MM231 - Temsirol. 50nM - WF
MM231 - Temsirol. 200nM -WF
Cell number (x10³)
Days
PF 20μM
p**= 0.01
C
Number of colonies/field
p ***= 0.0001
p ***= 0.0001
p ***= 0.0001
p **= 0.002
MM 453 CTR 10%FBS
MM 453 CTR 5%WF
MM453 p70KR 10%FBS
MM453 p70KR 5%WF
D
Percent of invading cells
p **= 0.003
MM 231 CTR 5% WF
MM 231 p70 KR 5% WF
MM 231 CTR PF 10μM
MM 231 CTR TEM 100 nM
E
Distance (mm from the edge of the drop)
p *= 0.015
MM 231 CTR 5% WF
MM 231 p70 KR 5% WF

Figure 3. Growth and motility of breast cancer cell lines is altered by impairing p70S6K activity.

A. Growth curve analysis of MDA-MB-231 CTR or p70KR cells. Cells have been seeded on day 0, in complete medium (CM) or in the presence of 3% wound fluids (WF), as indicated, and then counted by Trypan Blue exclusion test, every day for 5 days. **B.** Growth curve analysis of MDA-MB-231 cell line in the presence of the indicated inhibitors. Cells have been seeded in medium containing 3% wound fluids (WF) on day 0, in the presence of PF-4708671 (5 μM or 20 μM) or Temsirolimus (50 nM or 200 nM) or vehicle (untreated). **C.** Anchorage independent growth of MDA-MB-453 CTR or p70KR cells. Cells were included in soft agar in presence of complete medium (10% FBS) or 3% wound fluids (WF), for 3 weeks. Graph reports the count of colony number/field evaluated in each condition. **D.** Matrigel invasion assay of MDA-MB-231 CTR or p70KR cells or cells treated with the indicated inhibitor. Cells have been seeded on top of a transwell chamber, pre-coated with Matrigel, in the presence of 5% wound fluids (WF) plus PF-4708671 (10 μM) or Temsirolimus (100 nM), where indicated. The percent of invading cells after 12 hours is shown. **E**. Matrigel evasion assay of MDA-MB-231 CTR or p70KR cells. Cells were included in Matrigel in the presence of 5% wound fluids (WF) for 6 days, then fixed and analyzed for the distance covered from the edge of the drop.

In all the experiments, data represents the mean (± S.D.) of two independent experiments performed in triplicate. In all panels, statistical significance was calculated using the Student's t-test. A p value ≤ 0.05 was considered significant.

anchorage independent growth assays in soft agar, in the presence of either FBS or WF, we verified that impairment of p70S6K activity by expression of p70KR significantly decreased the cell ability to survive and grow (Figure 3C, CTR vs KR, in FBS p=0.002). In particular, when WF was used as source of survival and growth stimuli the difference was extremely significant (CTR *vs* KR, in WF p<0.0001). This suggested that, under this condition, the necessity for a robust p70S6K signaling was of particular relevance.

Then, we looked at the possibility that alteration of p70S6K activity could affect the migratory and invasive behavior of breast cancer cells. We challenged cells in three-dimensional (3D)-invasion or evasion assays, in order to more accurately mimic the *in vivo* microenvironment. Invasion of a 3D-matrix highlighted more significant differences between control cells and cells with impaired p70 signaling, particularly when p70S6K1, and not mTOR, was attacked (Figure 3D, CTR vs PF-treated p=0.003; Figure 3E, CTR vs KR p=0.015). Altogether, these results support the notion that p70S6K activity positively contributes to proliferation and invasion programs of breast cancer epithelial cells.

3.1.3. Impact of p70S6K activity on primary tumor growth.

To evaluate whether the impairment of p70S6K signaling would impact on breast tumorigenesis, we used an orthotopic xenograft model of breast cancer and injected MDA-MB-231 control- or p70KR-cells in mouse mammary fat pads (MFP) using Matrigel to support their initial survival. As expected, results indicated that, under these conditions, impaired p70S6K activity strongly decreased primary breast tumor growth (Figure 4A and data not shown). Next, we injected decreasing numbers of MDA-MB-231 control- or p70KR-cells and waited until tumors reached similar volumes before excising the masses. p70KR-cells grew slower and reached the same tumor mass approximately one week later respect to controls (data not shown). Then, in order to challenge their ability to initiate tumor growth in more stringent conditions and possibly discern among the ability of p70S6K signaling to impact on proliferation or survival of breast cancer cells *in vivo*, we injected decreasing cells number in MFP without Matrigel. It is interesting to note how in this setting, an intact p70S6K signaling was extremely critical for tumor initiation (67% versus 0%, in control- and p70KR-cells, at low cell number, $1x10^5$, n=12) (Figure 4B). More careful analysis of tumors arising from $2x10^5$ and $4x10^5$ injected cells suggested that impairment of p70S6K signaling significantly increased the tumor latency (9 versus 26 days, Figure 4C) but, once tumors appeared, their growth rate was very similar (Figure 4D). This observation pointed out that, in the process of tumor initiation, p70S6K signaling played a major role in survival rather than

A

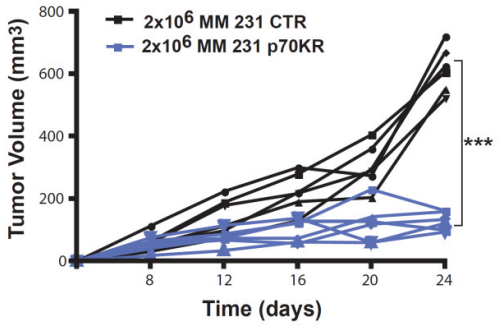

B

	# cells	MM231 CTR cells	MM231 p70KR cells
matrigel	2 x 10^6	6/6 100%	6/6 100%
	7.5 x 10^5	6/6 100%	6/6 100%
	2 x 10^5	6/6 100%	6/6 100%
	2 x 10^4	6/6 100%	6/6 100%
no matrigel	4 x 10^5	6/6 100%	6/6 100%
	2 x 10^5	6/6 100%	6/6 100%
	1 x 10^5	8/12 67%	0/12 0%

C

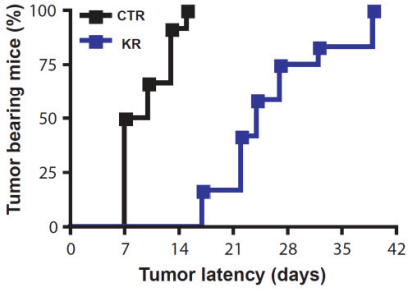

D

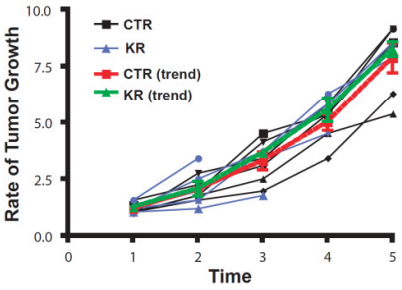

E

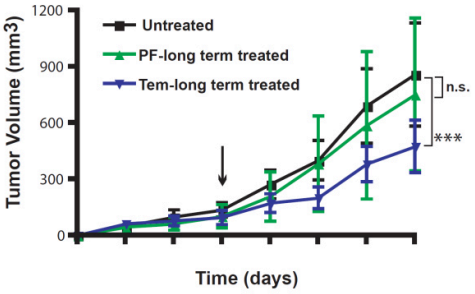

Figure 4. Primary tumor growth is altered by impairing p70S6K activity. A. Growth curves, expressed as tumor volume (mm^3), of primary tumors derived from injection of MDA-MB-231 cells ($1x10^6$) stably transduced with a retroviral empty vector (CTR) or with a retroviral vector encoding for a kinase inactive mutant of p70S6K (KR), in thoracic mammary fat pads of nude mice (2 MFP/mouse) in 50 µl Matrigel/PBS (1:1). Mice were sacrificed after 3 weeks. Statistical significance was calculated using the Student's t-test, pooling together values of the last measurement of controls vs p70KR. Three asterisks (***) indicate a p value ≤ 0.005. **B.** Tumor take-rate assessed by injection of the indicated numbers of MDA-MB-231 CTR or p70KR cells, in the presence or absence of Matrigel. **C.** Graph reports the time dependent appearance of primary tumors derived from injection of MDA-MB-231 CTR or p70KR cells ($2x10^5$and $4x10^5$) in the nude mouse mammary fat pads (2 MFP/mouse) without Matrigel. Mice were sacrificed 7 weeks after injection. **D.** Graph reports the rate of tumor growth, independently from the time of appearance, in mice described in (C). Values are expressed as ratio of the tumor volume over the value of 20 mm^3, considered as cut off. The red and the green lines represent the trend of growth of the MDA-MB-231 CTR and p70KR, respectively. **E.** Growth curves, expressed as tumor volume (mm^3), of primary tumors derived from injection of MDA-MB-231 control cells ($2x10^6$), in the thoracic mammary fat pads of nude mice (2 MFP/mouse). Mice were intraperitoneally injected with PF-4708671 (25mg/kg, i.e. 600µg/mouse) or Temsirolimus (12.5mg/kg, i.e. 300µg/mouse) or vehicle (untreated), twice a week for three weeks. Data represent the mean (± S.D.) of 10 tumors/treatment. Statistical significance was calculated using the Student's t-test, pooling together values of the last measurement. Three asterisks (***) indicate a p value ≤ 0.005. Difference in tumor volume between Untreated and PF-treated tumors was not significant (n.s.).

in proliferation of breast cancer cells. Next, to establish the role of p70S6K in a preclinical model, we used an alternative approach, mimicking a neo-adjuvant setting. We bilaterally injected MDA-MB-231 control cells in mouse MFP and, from appearance of a palpable mass, we treated mice with PF, Tems or vehicle twice a week, for three weeks. No particular sufferance or toxicity was observed during treatment, either with PF or Tems. In line with the established role of mTOR in cell growth, Tems treated mice displayed a considerable decrease in their tumor growth throughout the course of treatment (Figure 4E). Treatment with PF did not elicit a significant decrease in the growth of established primary tumors, indicating that specific p70S6K1 activity is not essential during this stage of tumorigenesis, in agreement with what observed using p70KR expressing cells (Figure 4C-D).

3.1.4. Impact of p70S6K activity on breast cancer local relapse.

The main goal of our study was to understand whether p70S6K played a role in the formation of breast cancer local recurrence. We designed an experimental model *in vivo* resembling the course of human breast cancer (Figure 5A). We bilaterally injected breast cancer cells in mouse MFP, waited for primary tumors to grow and surgically removed masses under anesthesia. After recovering, mice were followed up to detect manifestation of recurrence. After 8 weeks from surgery, mice were sacrificed and mammary glands, recurrences (if present) and lymphnodes were collected (Figure 5A). Since the impairment of p70S6K activity gave rise to smaller tumors (Figure 4A), we injected $1x10^6$ control cells (left MFP) and $2x10^6$ p70KR expressing cells (right MFP) in order to obtain, at surgery time, primary tumors of similar size and easily excisable (Figure 5B-C). Control mice showed a recurrence rate of 64% (Figure 5I). Strikingly, in p70KR-injected mice percentage of local relapse dramatically dropped to 18% (Figure 5I). Tumor spreading to loco-regional lymphnodes was detected only ipsilaterally to CTR cells-injected MFPs (Figure 5D). Similar results were obtained using MDA-MB-231 cells stably transduced with specific shRNA silencing p70 (Figure 5I). Importantly, PCR analyses have excluded the possibility that recurrences observed in the left MFP (injected with control cells) could be caused by p70KR expressing cells incidentally attracted to the surgery site from circulation (Figure 5E). Detection of strong and consistent increase of S6 phosphorylation in all relapses respect to paired primary tumors (Figure 5F) further supported that p70S6K signaling was relevant during this process.

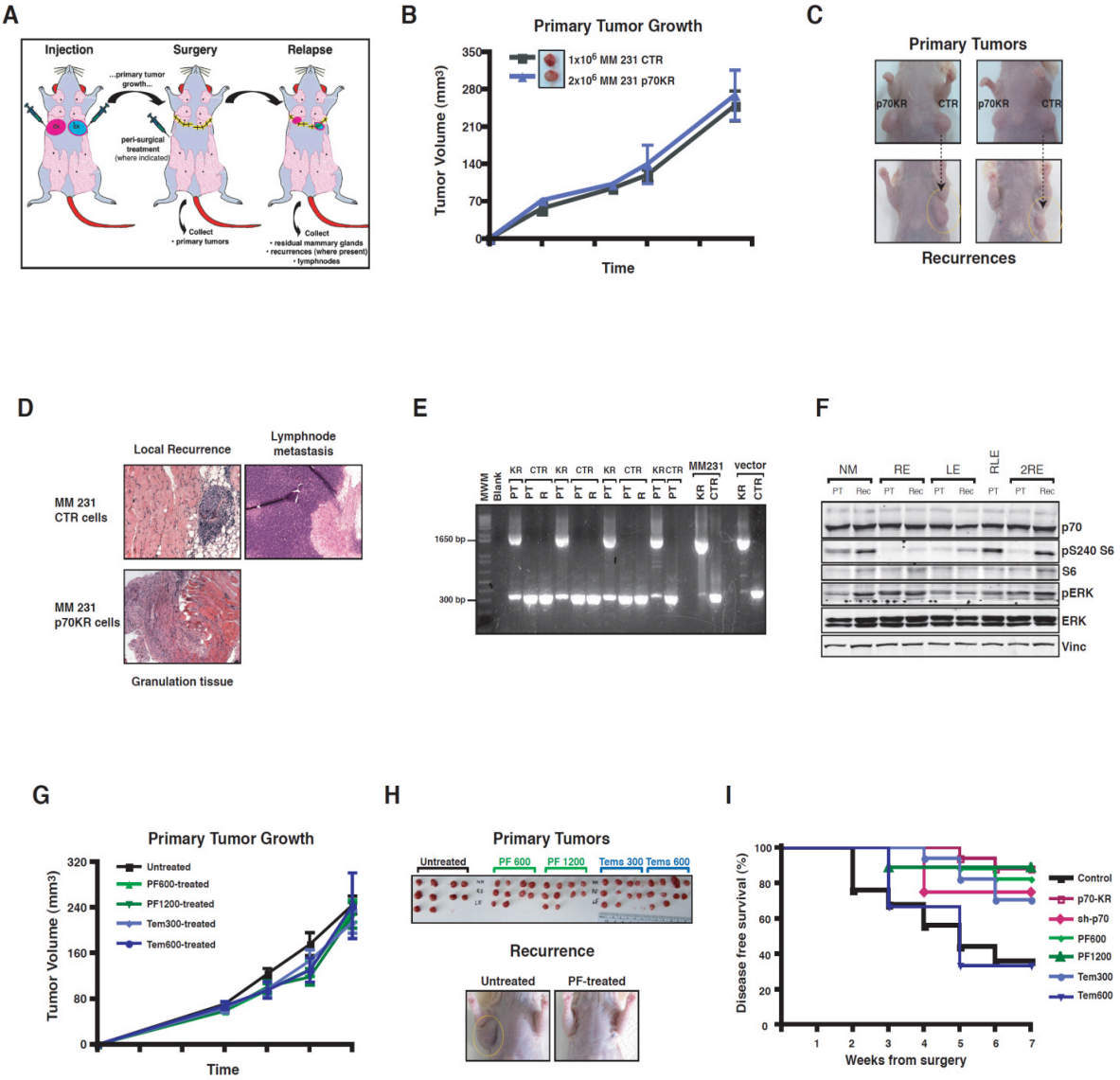
A
Injection
Surgery
Relapse
...primary tumor growth...
peri-surgical treatment (where indicated)
Collect
• primary tumors
Collect
• residual mammary glands
• recurrences (where present)
• lymphnodes
B
Primary Tumor Growth
1x10^6 MM 231 CTR
2x10^6 MM 231 p70KR
Tumor Volume (mm3)
350
280
210
140
70
0
Time
C
Primary Tumors
p70KR
CTR
p70KR
CTR
Recurrences
D
Local Recurrence
Lymphnode metastasis
MM 231 CTR cells
MM 231 p70KR cells
Granulation tissue
E
MWM
Blank
KR
CTR
MM231
vector
1650 bp
300 bp
F
NM
RE
LE
RLE
2RE
PT
Rec
p70
pS240 S6
S6
pERK
ERK
Vinc
G
Primary Tumor Growth
Untreated
PF600-treated
PF1200-treated
Tem300-treated
Tem600-treated
Tumor Volume (mm3)
320
240
160
80
0
Time
H
Primary Tumors
Untreated
PF 600
PF 1200
Tems 300
Tems 600
Recurrence
Untreated
PF-treated
I
Disease free survival (%)
100
80
60
40
20
0
1
2
3
4
5
6
7
Weeks from surgery
Control
p70-KR
sh-p70
PF600
PF1200
Tem300
Tem600

Figure 5. Local recurrence of breast cancer is prevented by impairing p70S6K activity. **A.** Schematic representation of the experimental design, set up to evaluate the appearance of breast cancer recurrences. **B.** Growth curves, expressed as tumor volume (mm^3), of primary tumors derived from injection of MDA-MB-231 CTR cells ($1x10^6$), in the left MFP or p70KR ($2x10^6$), in the right MFP of nude mice. Data represent the mean (± S.D.) of 5 tumors/cell type, measured during the time preceding surgery. **C.** Representative images of mice displaying similar size of primary tumors (upper panels) but resulting in the formation of local recurrence only in left MFP, injected with CTR cells (lower panels). **D.** Representative images of histo-pathological analysis of recurrences or residual mammary glands excised from mice described in (B), following haematoxylin and eosin staining. **E.** PCR on retro-transcribed RNA extracted from primary tumors and/or recurrences, as indicated, using primers designed on the retroviral vector encoding for p70KR (1600 base pair, bp). **F.** Western blot analysis of primary tumor lysates and corresponding recurrent disease lysates (where present) from experiment described in (C). Pt: primary tumor, Rec: recurrence. Vinculin was used as loading control. **G.** Growth curves, expressed as tumor volume (mm^3), of primary tumors derived from injection of MDA-MB-231 CTR cells ($2x10^6$), in nude mouse thoracic mammary fat pads. Mice were intraperitoneally injected with PF-4708671 (25mg/kg or 50mg/kg i.e. 600μg/mouse or 1200μg/mouse) or Temsirolimus (12.5mg/kg or 25mg/kg i.e. 300μg/mouse or 600μg/mouse) or vehicle (untreated). Treatments were administered three times following a "peri-surgical schedule". Data represent the mean (± S.D.) of 10 tumors/treatment. **H.** The picture above shows the primary tumors, excised the day of surgery, from mice described in (G). The pictures below show representative images of an untreated mouse displaying recurrent disease and a PF-treated mouse with no recurrence, 8 weeks after surgery. **I.** Graph reports the disease free survival in the indicated cohorts of mice, after removal of the primary tumor. Data are reported as percentage of mice that developed recurrent disease during the 8 weeks of follow up.

3.1.5. Peri-operative treatment with specific p70S6K1 inhibitor, but not with mTOR inhibitor, is sufficient to restrain breast cancer local relapse.

To exploit the possibility of therapeutically targeting p70S6K in breast cancer, we tested p70S6K1 specific inhibitor PF *in vivo* (119). In parallel, we also tested mTOR inhibitor Tems. We reasoned that restraining p70S6K activity during the surgery-induced inflammatory response would hamper residual cancer cells to locally survive and re-grow and, thus, we designed a three-days schedule of peri-operative treatment (day -1, day 0 and day +1, respect to surgery). We bilaterally injected MDA-MB-231 control cells in nude mice MFPs and, when primary tumors reached a volume of 200-300mm^3, we treated mice with vehicle, PF or Tems (Figure 5G-H). Peri-operative treatment with PF was highly effective in blocking the formation of recurrences (Figure 5I; 64% in controls vs 23% in PF600μg and 11% in PF1200μg). Intriguingly, Tems was ineffective or even harmful to the mouse (Figure 5I, 64% in controls vs 67% of Tems 600μg). Statistical analysis demonstrated that treatment with high doses of PF was significantly more effective than treatment with high doses of Tems in reducing local relapse (p=0.03 in Logrank test; Hazard Ratio 6.7; 95% Confidence Interval 1.1-56.1). Altogether, our *in vivo* experiments demonstrated that p70S6K signaling is involved in local relapse of breast cancer and its specific inhibition significantly reduces the appearance of breast cancer recurrence.

3.1.6. In human breast carcinomas p70S6K activity is increased by surgery.

Given the relevance of our findings in the mouse model, we were keen to assess whether these data could have a clinical validation. If p70S6K plays a critical role during the early phases of recovery after surgery, we could appreciate its activation by assessing p70S6K activity in breast cancer specimens taken very close in time from the moment of surgery. Thus, we scrutinized p70S6K activity (by immunohistochemical staining of phospho-S6 protein) in 26 paired breast cancer specimens from patients who undergone lumpectomy first and surgical widening to clear surgical margins in a second time (1-2 weeks later). By comparing phospho-S6 levels, we observed that nearly 50% of patients displayed an increase of p70S6K activity in the second specimen respect to the first and only 8% showed a reverse trend, thus strongly supporting the hypothesis that p70S6K activity is increased by surgery, also in human tissues (Figure 6).

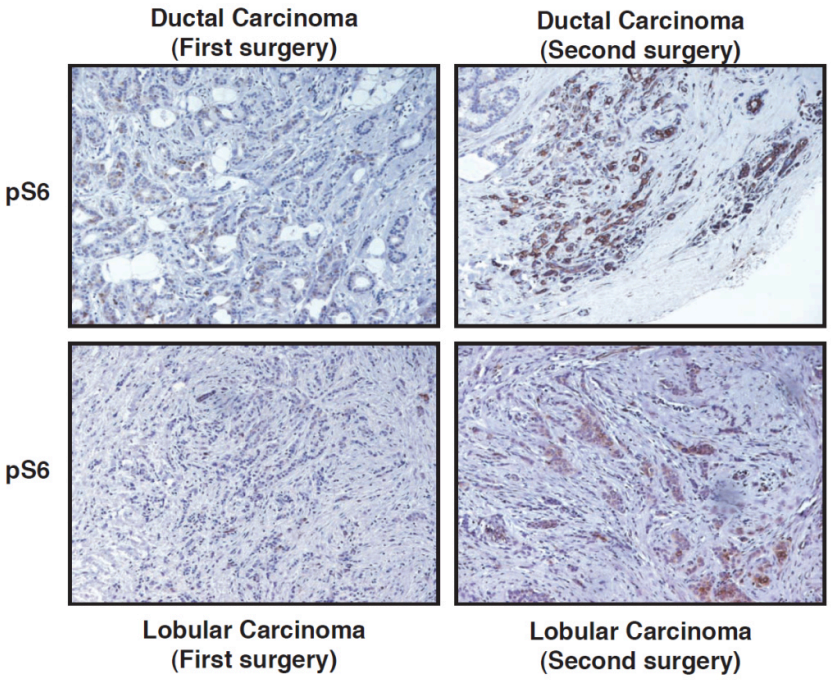
Ductal Carcinoma
(First surgery)
Ductal Carcinoma
(Second surgery)
pS6
pS6
Lobular Carcinoma
(First surgery)
Lobular Carcinoma
(Second surgery)

Figure 6. Human breast cancer display increased levels of p70S6K activity after surgery. Images of immunohistological analysis of phosphorylated S6 expression (pS240/244 S6), in samples from two representative breast cancer patients (ductal carcinoma, upper panels and lobular carcinoma, lower panels) who underwent second surgery, due to margin positivity.

3.1.7. p70S6K activity controls survival of breast cancer cells.

Results obtained so far suggested that a robust p70S6K signaling was necessary for residual isolated cells to survive in the breast microenvironment and to eventually recur. To understand the mechanism, we challenged cells to survive in anchorage independence, plating them on poly-HEMA coated dishes, and evaluated their survival at different time points. TUNEL assay and FACS analysis of active caspase 3/7 were then performed, revealing a significant difference in the apoptotic rate anytime p70S6K signaling was tackled (Figure 7A-B and data not shown). Although an increase in apoptosis was underscored, the use of Tems was not as effective as PF (Figure 7A-B and data not shown). Since it is known that prolonged treatment with mTOR inhibitors leads to hyper-activation of AKT (76), we tested whether failure of Tems treatment in our model could be linked to an AKT-mediated survival response. Our results indicated that Tems treatment, initially efficient in dampening p70S6K signaling, soon led to AKT hyper-activation (Figure 7C). Conversely, PF maintained its inhibition on p70S6K signaling also at longer times, without affecting AKT activation (Figure 7C). To get more molecular insights, we performed a phosphoproteomic array comparing the levels of activation and/or expression of more than 500 proteins in Tems-treated cells respect to PF-treated ones. Normalized data confirmed the hyper-activation of AKT and highlighted the contextual up-regulation of the pro-survival protein Bcl2 (data not shown). Western Blot analysis of cells exposed to increasing doses of Tems uncovered a dose-dependent AKT activation, coupled with phosphorylation of its downstream target FOXO3A and up-regulation of Bcl2 (Figure 7D). These findings prompted us to verify whether these molecular events occurred *in vivo*, as well. We bilaterally injected mouse MFPs with MDA-MB-231 cells and, when palpable masses appeared, treated tumors for three consecutive days with vehicle, PF or two different doses of Tems (6 tumors/treatment). Then, mice were sacrificed and tumors analyzed. Also in this context, AKT hyper-activation coupled with Bcl2 up-regulation were consistently detected in Tems-treated tumors (Figure 7E-G). Notably, staining of Bcl2, either by IF or by IHC, highlighted a specific and discrete pattern of expression inside the tumor, with agglomerations of Bcl2-positive cells immersed in a Bcl2-negative mass. This finding suggested that, under prolonged Tems treatment, isolated cells activated asurvival response that could eventually be responsible for the high rate of local relapse observed in Tems-treated mice.

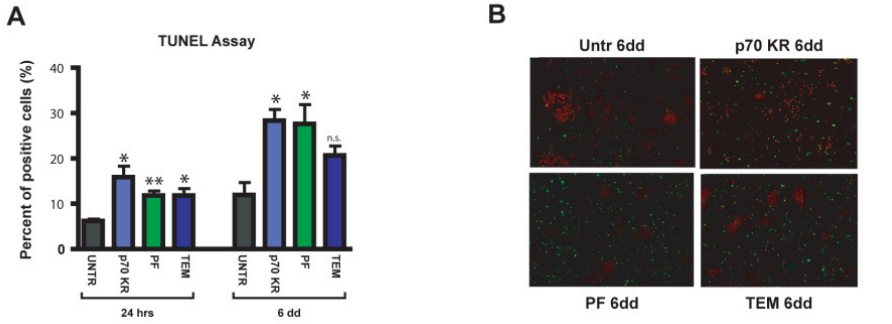
A
TUNEL Assay
Percent of positive cells (%)
40
30
20
10
0
UNTR
p70 KR
PF
TEM
24 hrs
6 dd
n.s.
B
Untr 6dd
p70 KR 6dd
PF 6dd
TEM 6dd

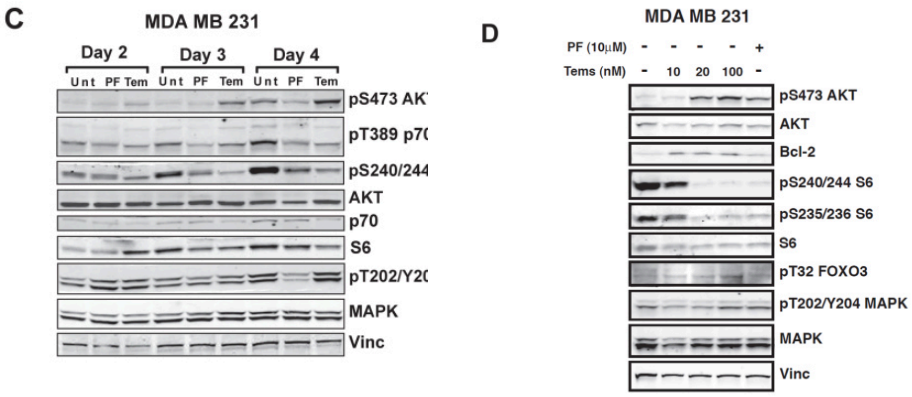
C
MDA MB 231
Day 2
Day 3
Day 4
Unt PF Tem Unt PF Tem Unt PF Tem
pS473 AK
pT389 p7
pS240/244
AKT
p70
S6
pT202/Y2
MAPK
Vinc
D
MDA MB 231
PF (10μM) - - - - +
Tems (nM) - 10 20 100 -
pS473 AKT
AKT
Bcl-2
pS240/244 S6
pS235/236 S6
S6
pT32 FOXO3
pT202/Y204 MAPK
MAPK
Vinc

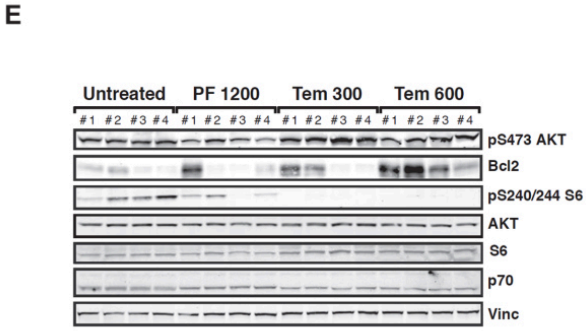
E
Untreated
PF 1200
Tem 300
Tem 600
#1 #2 #3 #4 #1 #2 #3 #4 #1 #2 #3 #4 #1 #2 #3 #4
pS473 AKT
Bcl2
pS240/244 S6
AKT
S6
p70
Vinc

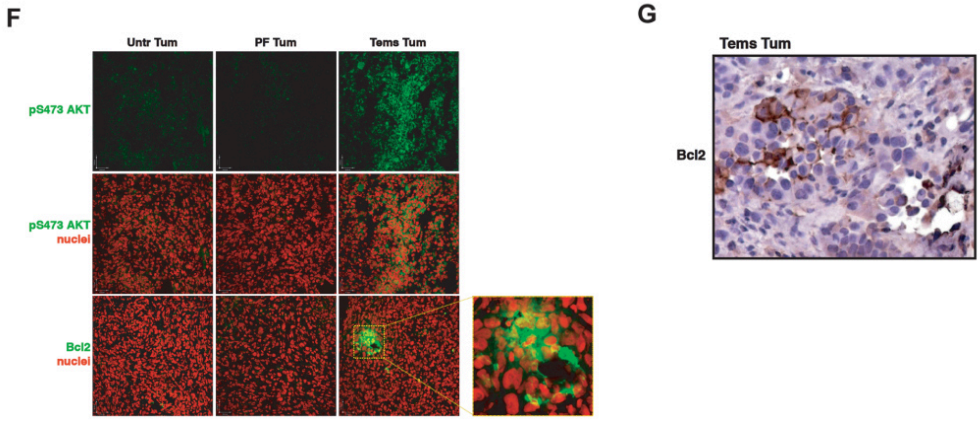
F
Untr Tum
PF Tum
Tems Tum
pS473 AKT
pS473 AKT
nuclei
Bcl2
nuclei
G
Tems Tum
Bcl2

Figure 7. p70S6K activity controls survival in breast cancer cells.

A. TUNEL assay of MDA-MB-231 CTR, p70KR cells or treated with the indicated inhibitor (PF-4708671 10 μM or Temsirolimus 100 nM), grown in anchorage independence on poly-HEMA coated dishes for the indicated times. Data are expressed as percent of TUNEL-positive cells, obtained counting at least 1500 cells/time point/cell type. **B.** Representative images of TUNEL-stained cells, cytospinned on slides after 6 days of anchorage independent growth in poly-HEMA coated dishes. **C.** Western blot analysis of MDA-MB-231 cells grown for the indicated times in the presence of the indicated inhibitor. Vinculin expression was used as loading control. **D.** Western blot analysis of MDA-MB-231 cells treated with the indicated inhibitor (PF-4708671 10 μM or Temsirolimus 10, 20 and 100 nM) or left untreated. Vinculin expression was used as loading control. **E.** Western blot analysis of lysates derived from primary tumor from MDA-MB-231 control cells. Mice were intraperitoneally injected with PF-4708671 (50mg/kg i.e. 1200μg/mouse) or Temsirolimus (12.5mg/kg or 25mg/kg i.e. 300μg/mouse or 600μg/mouse) or vehicle (Untreated) for three consecutive days and then sacrificed. **F.** Immunofluorescence analysis on tumor sections from experiment described in (E), acquired by confocal microscopy. Panels show: immunostaining for pS473 AKT (AF-488, green), immunostaining for pS473 AKT (AF-488, green) with the nuclear staining with propidium iodide (red) and the merge of the immunostaining for Bcl2 (AF-488, green) with propidium iodide (red). Bars correspond to 35 μm. **G.** Immunohistochemistry analysis of Bcl2 on tumor section from a Tems-treated mouse of the experiment described in (E). Nor untreated tumors nor those from PF-treated mice displayed positivity for Bcl2 (magnification 200x).

3.2. Role of STAT3 signaling pathway in breast cancer recurrence

3.2.1. STAT3 is strongly activated upon WF stimulation

WF are extremely rich in cytokines and growth factors and they have been used throughout the *in vitro* experiments of this project as surrogate source of the inflammatory stimuli present in the post-surgical setting in breast microenvironment. Our previous work demonstrated that they efficiently stimulated the activation of STAT3 in breast cancer cells, so, first of all, we evaluated the activation of STAT3 in a large panel of breast cancer cell lines (Figure 8A-B). We confirm that WF strongly activates STAT3 in all the cell lines tested (Figure 8A-B), it is evident that 5% WF is able to activate STAT3 at very higher extent than 10% FBS. These results suggest that an efficient stimulation of STAT3 is induced particularly in the presence of post-surgical fluids, indicating a specific role of STAT3 signaling pathway in this context.

STAT3 belongs to a family of signal transducers and transcription factors which consist in at least seven different members. We evaluated whether other members of STAT family were activated upon WF stimulation. Taking advantage of an immunoassay based on the Luminex techonology, we detected the activation of several members of STAT family upon WF stimulation. As indicated in the table (Figure 8C), this assay confirmed the data obtained by western blot: the phosphorylation of Y705 of STAT3 is strongly increased by stimulation of BC cells with WF (fold increase: 3.66). Among the other STAT proteins analyzed, only STAT1 was efficiently activated, but with a lesser extent respect STAT3. Thus, drainage WF strongly stimulate the activation of STAT3.

3.2.2. WF stimulate self-renewal in breast cancer cells

The signaling pathway of STAT3 is described to be involved in the growth and maintenance of tumor initiating cell (TICs) and to be important for self-renewal in breast cancer cells (110-113). We hypothesized that STAT3 could have an impact in the promotion of the survival and proliferation of TICs at the moment of surgical excision, when in the breast microenvironment are released factors that activate this pathway. First, we analyze whether drainage from breast cancer patients could activate the proliferation and self-renewal of TICs. As first approach, we evaluated the presence of side population in MCF-7 cells in the presence of WF. Side population is a small population of cells from cancer cell lines enriched in TICs, characterized by ability to exclude dyes such as Hoechst. FACS analysis revealed that the prolonged presence of WF strongly increase the percentage of side population in this cells, from 4.5% to 15.9% (Figure 9A).

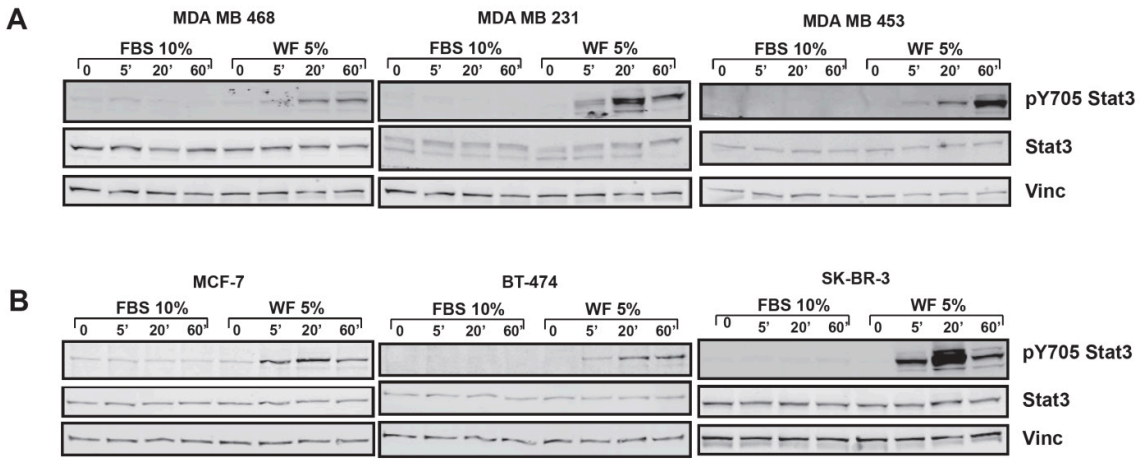

C

	pY701 STAT1	pY690 STAT2	pY705 STAT3	pY694/Y699 STAT5A/B	pY641 STAT6
UNSTIMULATED	9	8	51	27	7
STIMULATED	25,5	12	186,5	27	7
FOLD INCREASE	2,83	1,5	3,66	1	1

Figure 8. In breast cancer cell lines, STAT3 is strongly activated following stimulation with wound fluids.

A. Western blot analysis of MDA-MB-468, MDA-MB-231 and MDA-MB-453 cell lines serum starved and then stimulated for the indicated times with 10% serum (FBS) or 5% wound fluids (WF). **B.** Same as in (A), but using MCF-7, BT-474 and SK-BR-3 cell lines, as indicated. Vinculin expression was used as loading control.**C.** Table reports the activation of five different members of STAT family in MDA-MB-231 cells, following stimulation with 5% wound fluids for 20 minutes (stimulated) or not (unstimulated). Activation was detected using a commercial immunoassay. The value of "fold increase" represents the ratio between the unstimulated and stimulated values.

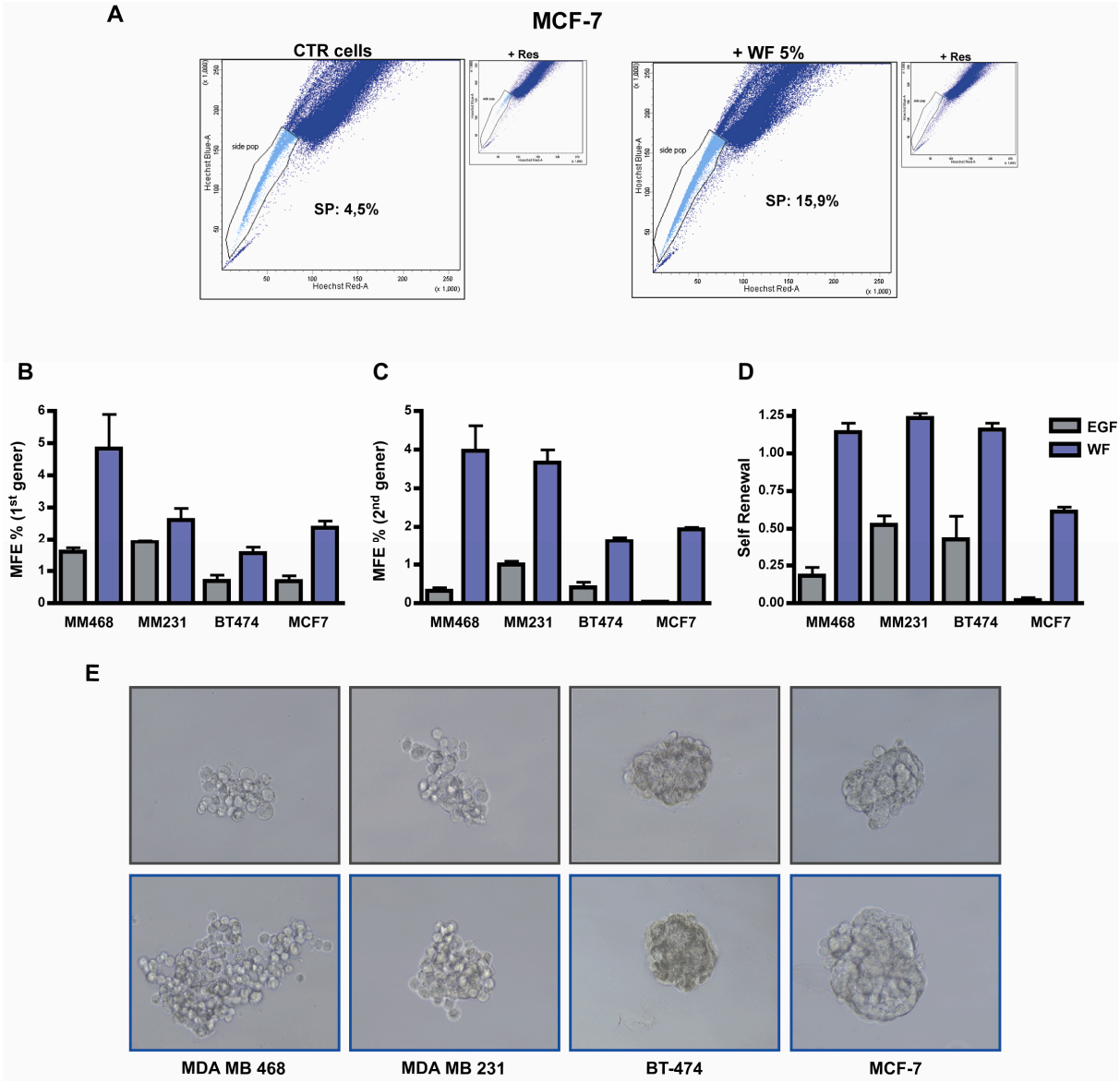
A
MCF-7
CTR cells
+ Res
+ WF 5%
+ Res
side pop
SP: 4,5%
SP: 15,9%
Hoechst Blue-A
Hoechst Red-A
B
MFE % (1st gener)
C
MFE % (2nd gener)
D
Self Renewal
EGF
WF
MM468
MM231
BT474
MCF7
E
MDA MB 468
MDA MB 231
BT-474
MCF-7

Figure 9. WF stimulate proliferation and self-renewal of tumor initiating cells.

A. FACS analysis evidences side population (SP) in MCF-7 cells growth in complete medium (CTR cells) or growth in the presence of wound fluids for 48 hours (WF 5%). SP is identified through exclusion of Hoechst dye that is inhibited in the presence of Reserpine. Percentage of SP is reported inside the plot. **B.** Graph reports mammosphere forming efficiency of MDA-MB-468, MDA-MB-231, BT474 and MCF7 cells. Cells were plated on poly-HEMA coated dishes in mammosphere medium (EGF) or without EGF but with the supplement of WF 5%. Mammosphere forming efficiency (MFE) was calculated as the ratio between the number of mammospheres counted per well and cells seeded per well. **C.** Same as in A but regarding the secondary generation of mammospheres formation. Mammospheres formed in the primary generation were collected, digested and replated as single cells in the medium described. **D.** Self-renewal in MDA-MB-468, MDA-MB-231, BT474 and MCF7 cells. Self-renewal was calculated as the ratio between the total number of the secondary mammospheres generated and the total number of primary mammospheres. In all the cell lines tested, only in the presence of WF self-renewal is stimulated. **E.** Representative pictures show the mammospheres formed by MDA-MB-468, MDA-MB-231, BT474 and MCF7 cells in the secondary generation.

To better characterized the possible role of WF in the stimulation of TICs proliferation and self-renewal, we perform the mammosphere assay (Figure 9B-E) that is recognized to be an important tool to quantify both stem cell activity and stem cell self-renewal. Stem cell activity is calculated from primary mammosphere formation as percentage of mammosphere forming efficiency (MFE, the ratio between the number of mammospheres counted per well and cells seeded per well), the self-renewal is obtained as the ratio between the total number of secondary mammospheres and the total number of primary mammospheres generated (119). We tested the ability of several breast cancer cells to form mammospheres plating them in standard mammospheres media (with EGF) or in the same media without EGF but with 5% WF. Our data indicate that we are able to obtain mammosphere formation in all the cell lines tested (Figure 9B-E). The presence of WF increase the MFE comparing with standard condition and more importantly the self-renewal is strongly promoted only when WF is added. Our results show that WF is able to efficiently stimulate the cancer initiating cells activity and self-renewal.

3.2.3. Generation and characterization of breast cancer cell lines with altered STAT3 activity

Our data indicate WF are able to strongly stimulate STAT3 activity and to induce breast cancer self-renewal. To study the role of STAT3 in the regulation of TICs mediated by WF *in vitro* and in the process of insurgence of local recurrence *in vivo,* we generated breast cancer cell lines with impaired STAT3 activity through different approaches. First, we down-modulates the activity of STAT3 in two triple negative breast cancer cell lines, MDA-MB-231 and MDA-MB-468 (Figure 10 and data not shown). We silenced endogenous STAT3 with anti-human STAT3 sh-RNA and verified the expression/activity of STAT3, especially in the presence of WF (Figure 10A and data not shown). STAT3 protein is efficiently silenced while the other pathways analyzed were unvaried. Importantly, the activity of STAT3 in the silenced clones remains strongly down-modulated respect the control also upon WF stimulation (Figure 10A). Then, we better characterized the behavior of STAT3-silenced cell lines. First, we stimulated the cells with WF and analyzed the expression of some of the STAT3 known target genes. qRT-PCR analysis evidences that, among the target genes analyzed, two are specifically down-regulated in sh-clones in the presence of WF, Bcl-2 and Survivin (Figure 10B). These results indicate that the survival response could be important for breast cancer cells in this context.

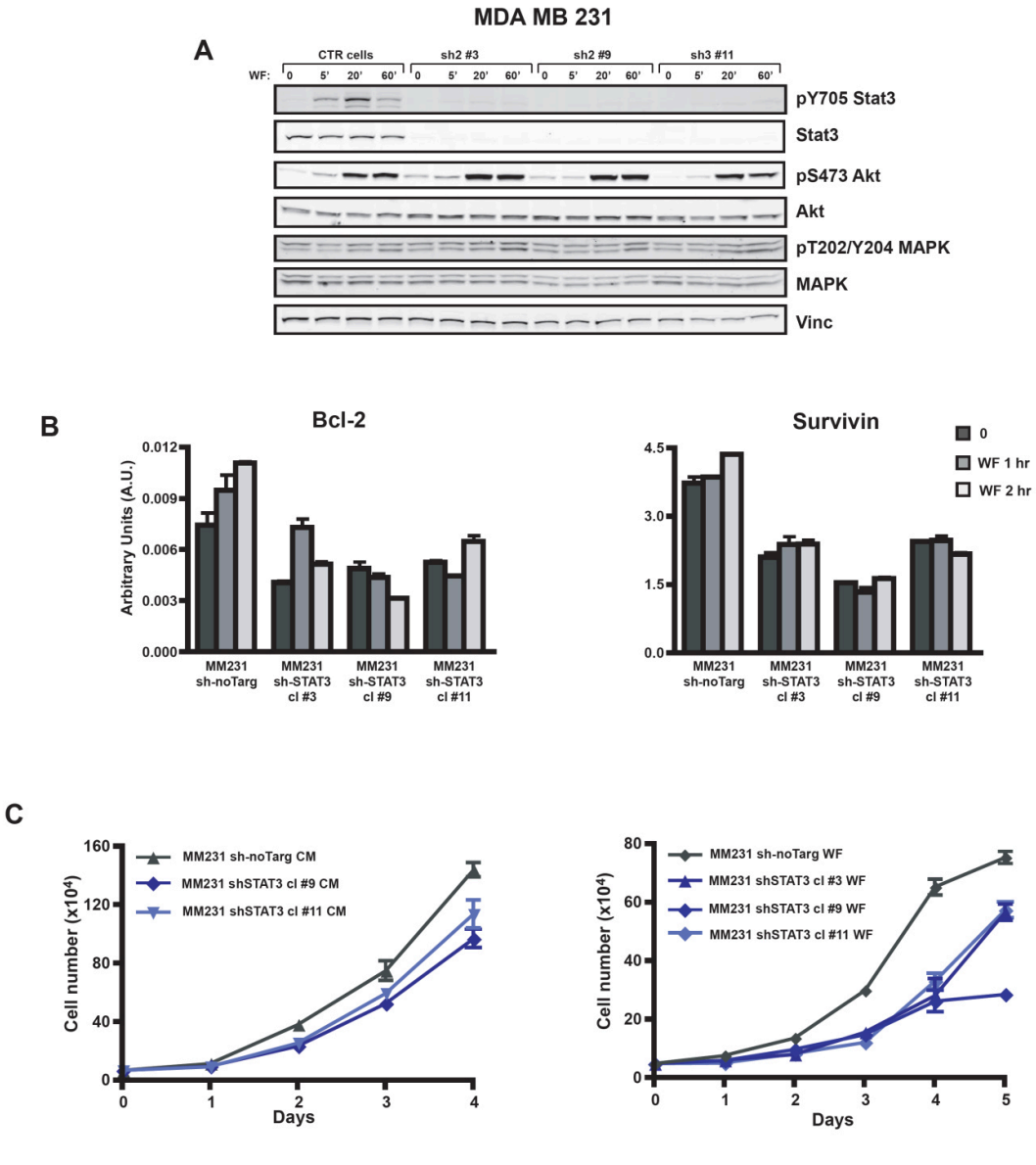
MDA MB 231
A
CTR cells
sh2 #3
sh2 #9
sh3 #11
WF: 0 5' 20' 60' 0 5' 20' 60' 0 5' 20' 60' 0 5' 20' 60'
pY705 Stat3
Stat3
pS473 Akt
Akt
pT202/Y204 MAPK
MAPK
Vinc
B
Bcl-2
Arbitrary Units (A.U.)
0.012
0.009
0.006
0.003
0.000
MM231 sh-noTarg
MM231 sh-STAT3 cl #3
MM231 sh-STAT3 cl #9
MM231 sh-STAT3 cl #11
Survivin
4.5
3.0
1.5
0.0
0
WF 1 hr
WF 2 hr
C
Cell number (x10⁴)
160
120
80
40
0
MM231 sh-noTarg CM
MM231 shSTAT3 cl #9 CM
MM231 shSTAT3 cl #11 CM
Days
0 1 2 3 4
80
60
40
20
0
MM231 sh-noTarg WF
MM231 shSTAT3 cl #3 WF
MM231 shSTAT3 cl #9 WF
MM231 shSTAT3 cl #11 WF
0 1 2 3 4 5

Figure 10. Activation of STAT3 following WF stimulation is efficiently impaired in breast cancer cell lines modified for STAT3 expression.

A. Western blot analysis of MDA-MB-231 cell line stably transduced with a lentiviral vector encoding for control sh-RNA (CTR) or for sh-RNAs directed against human STAT3 (sh), serum starved and then stimulated for the indicated times with wound fluids (WF). Vinculin is used as loading control. **B.** qRT-PCR analysis of Bcl-2 and Survivin expression in MDA-MB-231 CTR cells (sh no Target) or in three different silenced clones (cl#3, cl#9, cl#11). Cells were serum starved and then stimulated for the indicated times with wound fluids (WF). **C.** Growth curve analysis of MDA-MB-231 CTR or sh-STAT3 clones. Cells have been seeded on day 0, in complete medium (CM) or in the presence of 3% wound fluids (WF), as indicated, and then counted by Trypan Blue exclusion test, every day for 5 days.

The clones obtained were tested also in more functional assay. We analyzed the effects of alteration of STAT3 activity in the proliferative behavior of cells through growth curve assay. The proliferation rate of silenced cells is slightly decreased respect the control cells(Figure 10C). This is more evident when cells are cultured in the presence of 3% WF, suggesting that STAT3 activity could be more important in the regulation of breast cancer cells behavior when stimulated with inflammatory fluids (Figure 10C).

As second approach, we impaired STAT3 activity through the use of several different commercially available chemical inhibitors. We chose to use four inhibitors, differing for their mechanism of action: S3I-201, Stattic and STA-21 are non-peptidic inhibitors targeting SH2 domain and Galiellalactone, targeting the DNA binding domain. To obtain the inhibition of STAT3 activity and to avoid tossicity of the chemical compounds, we first set up the optimal concentration and the time of treatment for each cell line. We performed differential separation of cytoplasmic and nuclear fraction to analyze the activity and nuclear translocation of STAT3 in the presence or not of the inhibitors (Figure 11A). S3I-201, Stattic and STA-21 are described to target the SH2 domain of STAT3, thus preventing its nuclear translocation. From western blot analysis we could appreciate that S3I-201, Stattic and STA-21 were able to inhibit the shuttling of STAT3 from cytoplasm to nucleus after WF stimulation. STA-21 and S3I partially affect the expression of Cyclin D1, one of the targets of STAT3 (Figure 11A). Regarding the effect of Galiellalactone, as expected, the translocation of STAT3 in the nucleus was not affected (Figure 11A). We evaluated also whether the inhibitors used impaired the expression of STAT3 target genes, at RNA level. In MDA-MB-468 cells all inhibitors were quite effective in decreasing the expression of Bcl-2, Survivin and Cyc D1 (Figure 11B). In MDA-MB-231 cells the effect of the different compounds on the expression of these genes although present was less evident (Figure 11B). Our data show that S3I, Stattic and STA-21 were quite effective in preventing the translocation in the nucleus and the activation of STAT3 in both the cell lines. Galiellalactone seemed to be more efficacious in MDA MD 468 cells where it inhibited all target genes analyzed.

3.2.4. Inhibition of STAT3 impairs mammosphere formation and self-renewal.

Our experiments indicate that WF induce mammospheres formation and increase self-renewal in breast cancer cells (Figure 9). Since it is well established that STAT3 is involved in the maintenance of stem-like properties of breast cancer cells, we hypothesized that STAT3 could be a mediator of TICs properties induced by WF. To evaluate this possibility, we performed mammosphere assay plating the cells with medium containing 5% WF, in the presence or

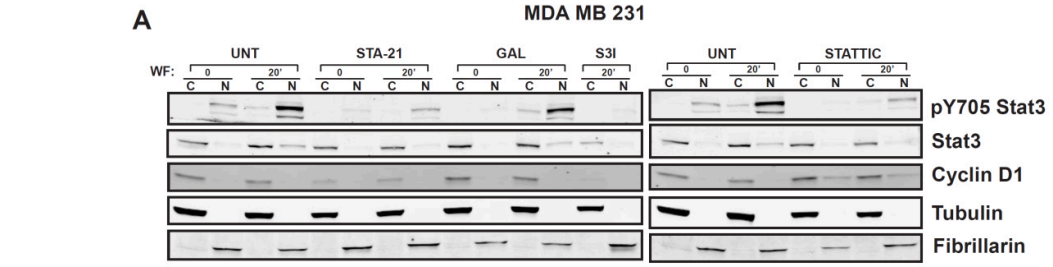
A
MDA MB 231
UNT
STA-21
GAL
S3I
UNT
STATTIC
WF:
0
20'
C
N
pY705 Stat3
Stat3
Cyclin D1
Tubulin
Fibrillarin

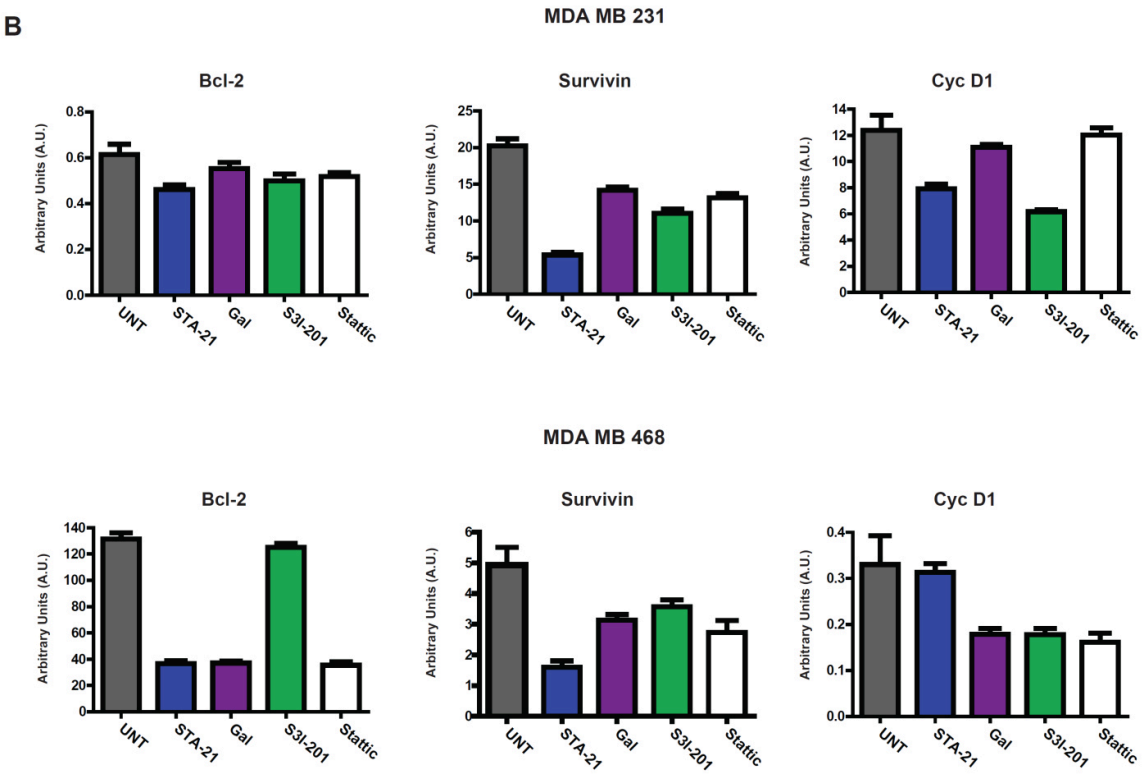
B
MDA MB 231
Bcl-2
Survivin
Cyc D1
Arbitrary Units (A.U.)
UNT
STA-21
Gal
S3I-201
Stattic
MDA MB 468
Bcl-2
Survivin
Cyc D1
Arbitrary Units (A.U.)
UNT
STA-21
Gal
S3I-201
Stattic

Figure 11. Activation of STAT3 following WF stimulation is efficiently impaired in breast cancer cell lines inhibited for its activity.

A. Western blot analysis of cytoplasmic and nuclear fraction in MDA-MB-231 cell line treated with STA-21 (30μM for 48h), Galiellalactone (12μM for 3h), S3I-201 (50μM for 24h) and Stattic (10μM for 3h) or left untreated and stimulated for 20 minutes with 5% WF. Tubulin is used as cytoplasmic marker, fibrillarin as nuclear marker. **B**. qRT-PCR analysis of Bcl-2, Survivin and Cyclin D1 expression in MDA-MB-231 and MDA-MB-468 treated with STA-21, Galiellalactone, S3I-201 and Stattic or left untreated.

absence of the inhibitors previously characterized. In order to have multiple approaches and to have more robust results, we used all the compounds previously tested. All inhibitors had a strong effect in preventing the formation of mammospheres in all tested breast cancer cell lines (Figure 12A-D). In particular, we observed a dramatic effect in MDA-MB-468 cells, where the ability to form mammospheres is very high (MFE in WF: 7%). Not only the number but also the size of the mammospheres was affected (Figure 12C-D). Stattic inhibitor completely prevented the formation of mammospheres but we hypothesize a toxic effect of the compound in this context (Figure 12A-D). As additional approach, we used a blocking antibody for IL6, a cytokine known to activate STAT3 signaling pathway. The analysis of the mammospheres forming efficiency (MFE) value pointed out that the action of the blocking antibody only slightly impaired the formation of mammospheres in the cell lines tested, suggesting that blocking a single agent was not sufficient to inhibit the activation of STAT3 signaling in a medium rich of cytokines and growth factors such as WF (Figure 12A-D).

Then, we evaluated whether STAT3 activity in the presence of WF could be fundamental also in the process of self-renewal of cancer stem cells. Secondary generation of mammospheres could not be plated from cells derived from primary generation grown in the presence of inhibitors, due to the paucity and lower vitality of the mammospheres. So, we decided to plate the first generation in medium containing WF but without inhibitors that were added only in the secondary generation. Importantly, the graph show that the self-renewal of MDA-MB-468 cells is strongly affected by the inhibitors, supporting that STAT3 plays an important role in the promotion of renewal of TICs (Figure 12E).

Altogether, these data evidenced that WF strongly stimulated mammosphere formation and self-renewal of breast cancer cells and this is mediated, at least in part, by STAT3 .

3.2.5. STAT3 activity positively impacts on tumor take rate, *in vivo*

Once characterized the effects of inhibition of STAT3 in proliferation and mammosphere formation, *in vitro*, we moved to *in vivo* models. First of all, we evaluated whether the down-modulation of STAT3 activity could have a role in the initiation of primary tumors formation, in nude mice. We injected in mouse mammary fat pads decreasing number of MDA-MB-231control (CTR) cells and two different clones silenced for STAT3, using Matrigel to support their initial survival and waited for the appearance of tumor masses (Figure 13A-B). The take rate of CTR cells was 100%, injecting $2x10^5$, $1x10^5$ and $5x10^4$ cells while the behavior of the clones silenced for STAT3 was slightly different. One of the clones tested

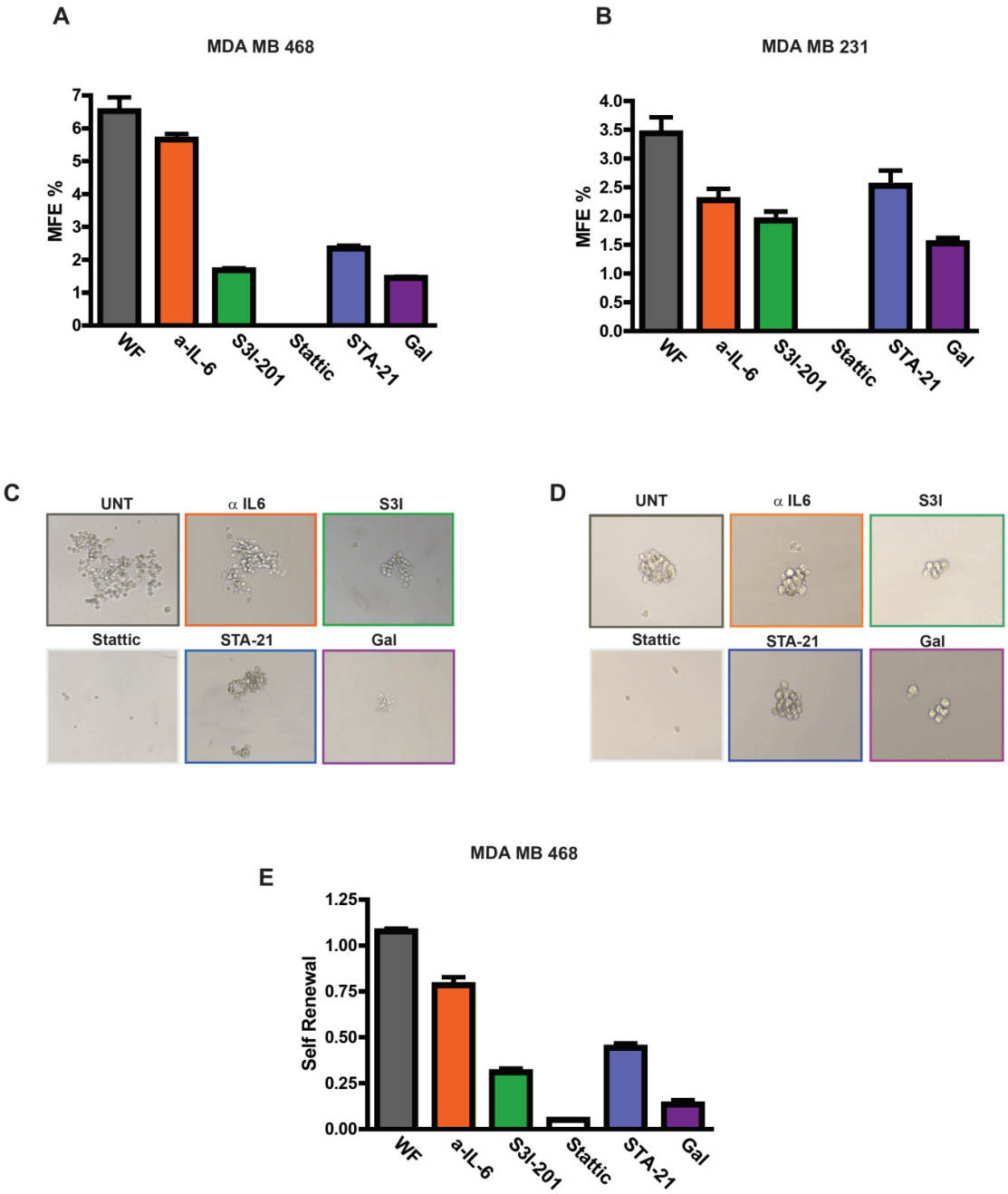
A
MDA MB 468
MFE %
WF
a-IL-6
S3I-201
Stattic
STA-21
Gal
B
MDA MB 231
MFE %
C
UNT
α IL6
S3I
Stattic
STA-21
Gal
D
E
MDA MB 468
Self Renewal

Figure 12. Inhibition of STAT3 impacts on maintenance and self-renewal of tumor initiating cells.

A. Graph reports mammosphere forming efficiency of MDA-MB-468 cells. Cells were plated on poly-HEMA coated dishes in mammosphere medium with the supplement of WF 5% in the presence or not of the indicated inhibitors(anti-IL6 0.2μg/ml, S3I-201 100μM, Stattic 10μM, STA-21 30μM and Galiellalactone 25μM). Mammosphere forming efficiency (MFE) was calculated as the ratio between the number of mammospheres counted per well and cells seeded per well. **B.** Same as in A but in MDA-MB-231 cells (anti-IL6 0.2μg/ml, S3I-201 50μM, Stattic 10μM, STA-21 30μM, Galiellalactone 12μM). **C.** Pictures show the mammospheres formed by MDA-MB-468 in the presence of STAT3 inhibitors. **D.** Same as in (C) but regarding MDA MD 231 cells. **E.** Graph reports self-renewal in MDA-MB-468 cells in the presence of the compounds indicated. Self-renewal was calculated as the ratio between the total number of the secondary mammospheres generated and the total number of primary mammospheres. Primary generation was obtained plating the cells on poly-HEMA coated dishes in mammosphere medium containing WF without the inhibitors. After the formation of mammospheres, cells were collected, digested and re-plated to form secondary mammospheres adding the inhibitors in the medium.

showed a decreased take rate but the other one, despite with a delay respect the CTR cells, showed a 100% take rate (Figure 13A). To evaluate more in detail these differences and to understand if it was a specific effect of STAT3 in the initiation of the tumors, we decided to inject lower numbers of cells to obtain a more stringent condition. Injecting $2x10^4$ and $1x10^4$, it is evident that imparing STAT3 activity strongly impacted on the tumor growth initiation (Figure 13A-B). At $2x10^4$ and $1x10^4$ cells, CTRs present a take rate of 88% and 50% respectively, while no tumor was formed by one of the 2 clones and only one tumor by the second clone (Figure 13A-B).

In conclusion, these data demonstrate that STAT3 activity positively impact on the initiation of breast tumorigenesis.

3.2.6. Role of STAT3 activity in the control of locoregional recurrence, *in vivo*

Our data suggested that STAT3 regulate TICs maintenance and self-renewal in the presence of WF and it is known that this population of cells is important for tumor recurrence. In order to evaluate the role of STAT3 in breast cancer local recurrence formation, we utilized an experimental model *in vivo*, already set up and characterized in our lab (Figure 5A). Since we know that primary tumors with impaired STAT3 grew less than the control (data not shown), we injected $1x10^6$ of MDA-MB-231 CTRs cells and $2x10^6$ of MDA-MB-231 sh-STAT3 clones, to obtain similar primary masses at the time of surgery. The picture in Figure 13C shows that the masses were very similar among the groups at the day of the surgery. These *in vivo* experiments are currently under evaluation. We monitor the appearance of local recurrence during a period of at least eight weeks. The data obtained so far (5 weeks) show STAT3 silencing decreased the number or recurrence formation from 56% in control mice to 25% for sh#9 and sh#11 (Figure 13D-E). The disease free survival at 5 weeks is positively affected by the inhibition of STAT3 activity (Figure 13E). However, long-term follow up is currently under way, to evaluate which is the actual involvement of STAT3 in the regulation of the processes that lead to local relapse.

A

# cells	MM231 CTR cells	MM231 sh#9 cells	MM231 sh#11 cells
2 x 10^5	2/2 100%	3/4 75%	N. A.
1 x 10^5	4/4 100%	2/4 50%	4/4 100%
5 x 10^4	4/4 100%	1/4 25%	4/4 100%
2 x 10^4	7/8 88%	0/8 0%	1/8 12%
1 x 10^4	4/8 50%	0/8 0%	1/8 12%

B

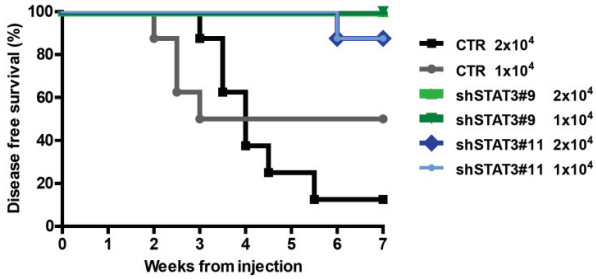

C

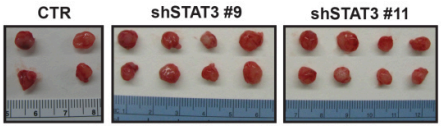

D

	% of recurrences
MM231 CTR cells	56%
MM231 sh#9 cells	25%
MM231 sh#11 cells	25%

E

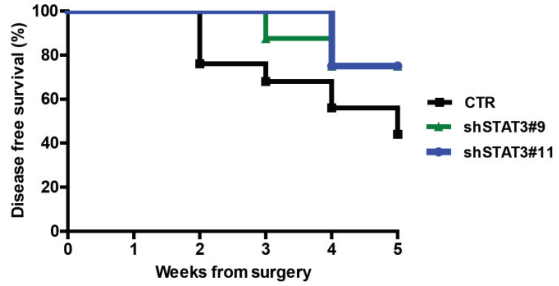

Figure 13. Impaired STAT3 activity decreases tumor take rate and recurrence formation in a mouse model of breast cancer.

A. Tumor take-rate assessed by injection of the indicated numbers of MDA-MB-231 CTR or sh-STAT3 clones, in the presence of Matrigel. **B.**Graph reports the disease free survival in the indicated cohorts of mice, after injection of decreasing number of MDA-MB-231 CTR or two different sh-STAT3 clones. Data are reported as percentage of mice that developed primary tumors during the 7 weeks of follow up.**C.** Figures show an example of primary masses excised from nude mice after surgery. It is evidenced the similar dimension of the tumors in the different groups. **D.** Table reports the percentage of local recurrences formed by mice injected with CTR cells or two different clones of sh-STAT3 after 5 weeks of follow up. Long-term follow up is currently in progress. **E.** Graph reports the disease free survival in the indicated cohorts of mice, after removal of the primary tumor. Data are reported as percentage of mice that developed recurrent disease during the 5 weeks of follow up. Long-term follow up is currently in progress.

4. DISCUSSION

Local relapse in EBC patients strongly influences disease outcome (11) and represents a common and unfavorable prognostic event. The preferential localization of breast cancer recurrences at the surgical scar site has not yet been adequately explained, and various hypotheses have been generated. The most common explanation is the presence of ‘‘residual’’ tumor cells after the surgical excision. However, this cannot be the unique reason. The possible deleterious effects of surgical wounding have been speculated for a long time and have been shown in mice (25,32). Also in humans, it was demonstrated that the growth kinetics of breast cancer micro metastasis is modified by surgery, representing a perturbing factor in the process of relapse or metastasis development (26, 31). Moreover, experimental and clinical observations suggest that the extent of surgery may represent a variable able to enhance tumor burden (24-26, 28, 121). A recent clinical study comparing radical mastectomy with breast conserving surgery reported that after extensive mastectomy, an excessive wound response during the healing process might stimulate the secretion of as-yet uncharacterized growth factor(s) that precipitates loco-regional recurrence (21). So, surgery and the consequent inflammatory response caused by wounding could be a factor that favors the proliferation of “residual” tumor cells. The communication between microenvironment and tumor cells plays an important role in this context. Normally, the microenvironment surrounding the tumor provides tumor-suppressive signals; however, once tissue homeostasis is lost, the altered microenvironment can itself become a potent tumor promoter, as amply demonstrated in recent research (121). The process of wound healing can provoke changes in the surrounding and shift the balance between tumor-suppressive and tumor-promoting signals. The combination of inflammation, growth factors produced in the microenvironment and other tissue-associated promotional forces can breach the barrier, resulting in promotion of the growth of residual cells into a tumor.

Interestingly, wound axillary fluids harvested from breast cancer patients have been proved to stimulate Her2-positive mammary carcinoma cell growth, an effect that could be only partially abrogated by impairing Her2 signal transduction (34). Accordingly, our previous work not only reveals that several growth factors and cytokines secreted in the WF participate in the stimulation of mammary carcinoma cells but also represents the first formal demonstration that WF harvested from breast cancer patients who have undergone wide local tumor excision stimulate breast cancer cell motility, invasion, and growth in three-dimensional contexts (33). In the same work we demonstrated that one single application of TARGeted Intraoperative RadioTherapy (TARGIT) almost completely abrogates the stimulatory effects of surgical WF on cancer cells *in vitro*, suggesting that it may confer more

benefits than those expected from the tumoricidal effect of radiotherapy (33). The beneficial effect of TARGIT could be attributed not only to a better cell killing but also by modifying the wound microenvironment. In support to this hypothesis the recent results of randomized trial TARGIT-A confirmed non-inferiority respect EBRT only when TARGIT was delivered concurrently with lumpectomy (prepathology stratum) but not in the postpathology stratum (35). Several factors might have played a part in achieving the low recurrence rates that was identified in the stratum randomized to receive TARGIT immediately after lumpectomy. These factors certainly include the immediate delivery of radiation to tissues, which appears to be essential to achieve the beneficial effects on the tumor microenvironment, suggesting that the timing of treatment is an important variable that can determine different clinical response (35). TARGIT significantly modifies the protein expression profile of the WF and the activation of p70S6 kinase and STAT3 pathways on stimulation of breast cancer cells (33).

In this work, we explore the role of p70S6K and STAT3 in the response to WF stimulation and in the process of breast cancer local recurrence. Many data suggest that p70S6K plays a pivotal role during breast cancer progression (33, 66-68, 70). Here, using a mouse model of EBC we show that interfering with p70S6K activity had a significant impact on breast cancer cell behavior and almost completely prevented formation of local recurrence. Importantly, a three-day schedule of peri-operative treatment with specific the p70S6K1 inhibitor PF-4708671 was sufficient to significantly prevent the appearance of relapses and our data demonstrate that this critical event takes place in very narrow window of the disease. Our data demonstrate that survival, more than proliferation, of residual isolated breast cancer cells requires the activity of p70S6K1. In accord with our data, a recent report demonstrated that p70S6K knock-down prevents lung metastasis in a breast cancer xenograft model (122), supporting that p70S6K is required for breast cancer cell settlement and survival. Inhibition of mTOR by Temsirolimus should, in principle, elicit the same response but our experiments clearly demonstrate that this is not the case. First, Tems did not induce a reduction of local recurrence rate in our mouse model of breast cancer. Then, Tems was not able to induce apoptosis in cells challenged to grow in anchorage independence. Finally, at molecular level, treatment with Tems blocked the p70S6K negative feedback loop, leading to activation of AKT and up-regulation of Bcl2, which, in turn, fostered cell survival. The activity of p70S6K is regulated by a wide range of extracellular signals and by multiple pathways (43,50). Although mTOR is the principal regulator of p70S6K, it is well documented that cooperation of upstream molecules is important for full activation and functionality of p70S6K (55, 123,

124) and targeting different nodes of the same pathway may result in dramatically different ability to block or promote a certain phenotype. This is strongly supported by our data showing that increasing doses of PF reduced recurrence formation, while increasing doses of Tems rather stimulated them. Very recent studies corroborate our finding. A kinome-wide drug profiling using a Drosophila model of multiple endocrine neoplasia type 2A, demonstrated that inhibition of S6K was required for optimal animal survival, whereas inhibition of Tor led to toxicity owing to release of negative feedback (125). In advanced prostate cancer, allosteric inhibition of mTOR by rapamycin was proved unable to achieve any therapeutic benefit (126), resulting in ineffective block of the translation of specific pro-invasion messenger RNAs, specifically mediated by its effector 4EBP1 and not p70S6K (126). In EBC, it is mandatory to restrain local recurrence (127, 128) because this will lead to one life saved every four recurrences prevented (11). In this context, targeting the pro-survival activity of mTOR by hampering p70S6K1 activity is necessary to cause breast cancer cell apoptosis and almost completely prevent cancer relapse.

STAT3 is inappropriately activated in a vast percentage of breast tumors but its concrete role in breast cancer initiation and/or progression is still very controversial. Here, we show that STAT3 was strongly activated when breast cancer cells were exposed to wound fluids (WF) drained from EBC patients, an experimental condition that partially contains and recapitulates *in vitro* the microenvironment surrounding cancer cells *in vivo*, following surgery. For the first time, we have shown here that prolonged stimulation with post-surgical fluids induces not only growth and invasion, but also the proliferation and self-renewal of breast cancer cells with phenotypes of tumor initiating cells. Our data indicate that in this process STAT3 signaling seems to be strongly involved. It is already known that STAT3 is an important regulator of tumor initiating cells that are known to be responsible for insurgence of cancer recurrences (108-113). By inhibiting STAT3 through different compounds, mammospheres formation induced by WF stimulation was strongly impaired; the same results were not achieved using an antibody able to block IL-6 signaling. WF is composed by a wide spectrum of cytokines and growth factors that are able to activate survival and proliferation by different intracellular signaling cascades. STAT3 pathway is certainly one of these cascades and its activation impinges on the TICs growth and maintenance. In accord with our results, other studies have shown that STAT3 is involved in regulation of TICs (108-113). Here, we not only confirmed these findings in our model system but we show that one of the possible effect of surgery on tumor cells is to increase “stemness properties” of breast cancer cells and that blocking STAT3 in this context could represent an exploitable strategy. The relevance of our

results *in vitro*, was confirmed by our results *in vivo*. The impairment of STAT3 pathway largely influenced the take rate ability of breast cancer cells in mouse MFP, especially when low numbers of cells were injected. It is known that STAT3 signaling is involved in inducing and maintaining a pro-carcinogenic inflammatory microenvironment (78). In line with this, inflammatory fluid produced after surgical excision activates STAT3 that induce proliferation of cells, leading to the appearance of local recurrence. Many of the downstream target genes of STAT3 encode cytokines and growth factors, the receptors of which signal through the same STAT3, thereby providing a mechanism for autocrine and paracrine STAT3 activation (78, 85, 88-90). It is possible that the activation of STAT3 by WF triggers a positive feedback loop that, not only activate the survival and proliferation of residual tumor cells but also activate the cells of the surrounding microenvironment, breaking the tissue homeostasis. It was shown that transient activation of Src can mediate a switch from immortalized breast cells to a stably transformed line that forms self-renewing mammospheres (129). This activation triggers a positive feedback loop mediated also by STAT3 that maintains the transformed state also in the absence of inducing signal. We can speculate that in our system, STAT3 activation could be a signal able to induce the transformation or the re-activation of cells that in absence of perturbing factors, such as surgery, will be dormant. The results obtained *in vitro*, prompt us to hypothesize that STAT3 could act specifically on tumor initiating cells, increasing the proliferation and the self-renewal ability already acquired or could stabilize cancer stem cell phenotype in residual cells. This possibility needs to be further explored and more time and experiments are now in progress to establish whether the specific inhibition of STAT3 could effectively represent a promising tool to restrain local recurrence.

The act of surgery leads to a profound modification of the local microenvironment. In that occasion reactive microenvironment is able to sustain the survival and, eventually, the re-growth of residual cancer cells through the secretion of inflammatory cytokines and growth factors. Altogether, our results allow to suggest that in this context two signaling pathways strongly influence the response of residual tumor cells. The activation of p70S6K1 prevalently impinges on the survival of these cells, while the activation of STAT3 stimulates the self-renewal ability of tumor initiating cells,which, we demonstrated here,is strongly promoted by WF. We can hypothesize that these pathways could cooperate to allow the growth of residual cells in this specific setting, to lead the formation of local relapse. Taken together, our findings provide a biological rationale for the use of molecularly targeted agents to compensate the harmful consequences of surgery and wound healing process. It is well

recognized that improved clinical efficacy of radiotherapy would make a substantive impact in clinical practice and patient outcomes (130). The use of peri-operative treatment with targeted agents in combination with intraoperative radiotherapy could improve the clinical response in EBC patients through the "sterilization" of microenvironment and the inhibition of the pathway mainly involved such as p70S6K and STAT3. The combination of treatments coupled with the correct timing of administration could strongly improve the patient response thus providing new therapeutic options also for the less responsive subtypes.

5. MATERIAL AND METHODS

5.1. Study approval

All animal experiments were reviewed and approved by the CRO Institutional Animal Care and Use Committee and were conducted according to that committee's guidelines.

Paraffin-embedded human breast cancer samples were obtained from the Università degli Studi di Roma La Sapienza, Azienda Ospedaliera Sant'Andrea, Rome, Italy.

Wound Fluids (WF) were collected at Centro di Riferimento Oncologico, Aviano, Italy.

Scientific use of biological material was approved by Ethics Committee of the Centro di Riferimento Oncologico, Aviano, and of Università degli Studi di Roma La Sapienza, Rome, Italy. Specific informed consent was obtained from all patients.

5.2. Cell culture and development of stable cell lines

MDA-MB-231 (basal, ER-, PR-, HER2-), MDA-MB-453 (luminal, ER-, PR-, HER2-), MDA-MB-468 (basal, ER-, PR-, HER2-), MCF-7 (luminal, ER+, PR+, HER2-), BT-474 (luminal, ER-, PR-, HER2+), BT-549 (basal, ER-, PR-, HER2-), HBL-100 (basal, ER-, PR-, HER2-) and SK-BR-3 (luminal, ER-, PR-, HER2+) mammary carcinoma cell lines (131) were obtained from ATCC (LGC Standards) and grown in Dulbecco modified Eagle medium (DMEM, Lonza) supplemented with 10% fetal bovine serum (FBS, SIGMA). Stable cell clones were obtained by retroviral transduction with a vector carrying Puromycin resistance (murine stem cell virus retroviral vectors, MSCV; Clontech), following the manufacturer's instructions, subcloned to encode for kinase inactive mutant HA-p70S6K-KR (carrying the substitution K100R) (117). The vector has been kindly provided by John Blenis (Harvard Medical School, Boston). p70S6K and STAT3-silenced mammary carcinoma cells were generated by lentiviral transduction of pLKO vectors encoding for human shRNAs of the MISSiON system (pLKO sh-p70S6K1: sh1_TRCN0000194766, sh2_TRCN0000003159, sh3_TRCN0000003162; pLKO sh-STAT3: sh2_TRCN0000020842, sh3_TRCN0000020843). All cell lines were authenticated by BMR Genomics srl Padova, Italia, on January 2012 according to Cell ID ™ System (Promega) protocol and using Genemapper ID Ver 3.2.1, to identify DNA STR profiles.

5.3. Preparation of protein lysates and immunoblotting analysis

MDA-MB-231, MDA-MB-453, MDA-MB-468, MCF-7, BT-474, BT-549, HBL-100 and SK-BR-3 mammary carcinoma cell lines were serum starved in DMEM containing 0.1% bovine serum albumin (BSA, SIGMA) and then stimulated with 10% FBS or 5% WF for the indicated time points. Where indicated, cells were also pre-treated for 30 minutes or for

longer times (as indicated) with the following inhibitors: PF-4708671 (p70S6K1 inhibitor, 10 μM, SIGMA) and Temsirolimus (Rapamycin analogue, 10, 20, 100 nM, Wyeth).

To extract total proteins cells were scraped on ice using cold NP40 lysis buffer (0.5% NP40; 50 mM HEPES pH 7; 250 mM NaCl; 5 mM EDTA; 0.5 mM EGTA, pH 8) plus a protease inhibitor cocktail (Complete™, Roche) and supplemented with 1 mM Na_3VO_4 (SIGMA), 10 mM NaF (SIGMA) and 1 mM DTT (SIGMA).

To extract total proteins from tumor specimens, the same procedure was used, except that tissue disruption was first achieved by using the TissueLyser II (Qiagen).

For immunoblotting analysis, proteins were separated in 4-20% SDS-PAGE (Criterion Precast Gel, Biorad) and transferred to nitrocellulose membranes (GE Healthcare). Membranes were blocked with 5% dried milk in TBS-0.1% Tween20 or in Odyssey Blocking Buffer (Licor, Biosciences) and incubated at 4°C overnight with primary antibodies. Then, membranes were incubated 1 hour at RT with horseradish peroxidase-conjugated secondary antibody (GE Healthcare) for ECL detection (GE Healthcare) or with IR-conjugated (Alexa Fluor 680, Invitrogen or IRDye 800, Rockland) secondary antibodies for infrared detection (Odyssey Infrared Detection System, Licor).

Primary antibodies AKT (sc-1618), ERK1 (sc-94), p70S6K1 (sc-8418), STAT3 (sc-482), Fibrillarin (sc-25397) and Vinculin (sc-7694) were purchased from Santa Cruz; pT202/204 ERK1/2 (#9101), pS473 AKT (#4060), pT389 p70S6K1 (#9234), S6 (#2217), pS235/236 S6 (#4858), pS240/244 S6 (#5364), pT37/46 4EBP1 (#2855), 4EBP1 (#9644), pT32 FOXO3a (#9464), pY705STAT3 (#9131) were purchased from Cell Signaling; Actin (#A5060) and Tubulin (T9026) was purchased from SIGMA; HA (#PRB101C) was purchased from Covance; Bcl2 (#OP60) was purchased from Calbiochem; Cyclin D1 (#04-1151) was purchased from Millipore.

5.4. Separation of nuclear and cytoplasmic fraction

MDA-MB-231 and MDA-MB-468 mammary carcinoma cell lines were serum starved in DMEM containing 0.1% bovine serum albumin (BSA, SIGMA) and then stimulated with 5% WF for the indicated time points. Where indicated, cells were pre-treated with the following inhibitors: STAT3 inhibitor VI S3I-20 (Santa Cruz; MDA-MB-231: 50μM with pre-treatment of 24h, MDA-MB-468: 100μM with pre-treatment of 24h), STA-21 (Santa Cruz; MDA-MB-231: 30μM with pre-treatment of 48h, MDA-MB-468: 30μM with pre-treatment of 48h), STAT3 inhibitor V Stattic (Santa Cruz; MDA-MB-231: 10μM with pre-treatment of 3h, MDA-MB-468: 10μM with pre-treatment of 16h) and Galiellalactone (Santa Cruz; MDA-

MB-231: 12 μM with pre-treatment of 3h, MDA-MB-468: 25 μM with pre-treatment of 24h). To perform the differential extraction of cytoplasmic and nuclear proteins, cells were resuspended in Buffer A (10 mM HEPES pH 7.9, 0.1 mM EDTA pH 8, 0.1 mM EGTA pH 8, 10 mM KCl) plus all the previously described inhibitors. Samples were kept on ice for 15 minutes, after that 0.5% NP40 was added and samples were centrifuged at 6000 rpm for 1 minute at 4°C. The supernatant, representing the cytoplasmic protein fraction, was collected. After three washes in Wash Buffer (0.32M sucrose, 3mM $CaCl_2$, 2mM Mg-Acetate, 0.1mM EDTA, 10mM Tris HCl pH8, 0.5% NP40), pellets were digested in Buffer C (20 mM HEPES pH 7.9, 1 mM EDTA pH 8, 1 mM EGTA pH 8, 400 mM NaCl, plus all the inhibitors) and incubated on ice for 20 minutes. Samples were then centrifuged at max speed for 15 minutes at 4°C to recover the supernatant, representing the nuclear protein fraction.

5.5. Wound fluid collection

Drainage Wound Fluids (WF) were collected over the 24h after surgery from unselected patients undergone breast-conserving surgery, as described previously (33). The assays were then performed using pools of all fluids.

5.6. Histological analysis and immunohistochemistry

Mouse samples were fixed in formalin (over night at 4°C) and processed for standard paraffin embedding. Histological sections (5μm thick) were made from the paraffin blocks, deparaffinated with xylene, and stained with haematoxylin and eosin.

For human breast cancer specimens, routine deparaffinization of all sections mounted on positive charge slides was carried out according to standard procedures, followed by rehydration through serial ethanol treatments. Slides were immersed in citrate buffer [0.01M sodium citrate (pH 6.0)] and heated in a microwave oven at 600W (three times for 5 min each) to enhance antigen retrieval. Endogenous peroxidase was blocked with 0.3% hydrogen peroxide in methanol for 30 min. Sections were immunostained for 1hr at room temperature with two different clones of anti-pS6 (#4858, #5364, Cell Signaling) or of Bcl2 (#OP60, Calbiochem). The primary antibody was omitted and replaced with preimmune serum in the negative control. Sections were reacted with biotinylated anti-rabbit antibody and streptavidin-biotin-peroxidase (Histostain-SP Kit, Zymed Laboratories, San Francisco, CA). Diaminobenzidine was used as a chromogene substrate. Finally, sections were washed in distilled water and weakly counterstained with Harry's modified haematoxylin.

5.7. Immunofluorescence analysis

Fresh mouse tumor specimens were included in OCT and stored at -80°C. Histological sections (5µm thick) were made from the OCT blocks and fixed 20' at RT in 4% PFA before blocking in 10% normal goat serum. Sections were immunoprobed at 4°C O.N. with anti-pS473AKT (#4060, Cell Signaling) or of Bcl2 (#OP60, Calbiochem) primary antibodies. The primary antibody was omitted and replaced with preimmune serum for the negative control. Sections were then probed with AlexaFluor-488-conjugated secondary anti-rabbit (Invitrogen) for 1h at RT, followed by nuclear staining with propidium iodide for 20' at RT. Stained sections were then observed using a confocal laser-scanning microscope (TSP2 Leica) interfaced with a Leica DMIRE2 fluorescent microscope.

5.8. Proliferation assays

For growth curve, 5-9 x 10^4 cells/well (depending on the cell type) were seeded in 6-well plates in complete medium or in serum free medium supplemented with 3% WF (SFM-3% WF), in triplicate. Where indicated, PF-4708671 (p70S6K1 inhibitor, SIGMA) or Temsirolimus (Rapamycin analogue, Wyeth) were added in the medium at the concentration indicated. Fresh medium, with or without inhibitors, was added every other day. At the indicated times, cells were detached by trypsin-EDTA and counted by Trypan Blue exclusion test.

To evaluate the anchorage-independent cell growth, MDA-MB-453 cells ($1.5x10^4$) were re-suspended in 2 ml top agar medium (DMEM-10% FBS or SFM-3% WF, 0.4% Low Melting Agarose, SIGMA) and quickly overlaid on a previously gelified 0.6% bottom agar medium (DMEM-10% FBS, 0.6% LowMelting Agarose, SIGMA). The experiments were performed in six-well tissue culture plates, in triplicate. Fresh medium was added to the wells twice a week as a feeder layer. After three weeks, the number of colonies was counted in 10 randomly chosen fields, at 10X magnification.

5.9. Motility assays

For invasion experiments, HTS Fluoroblok transwells were coated overnight at 4°C with a layer of Matrigel (6µg, Cultrex BME) diluted inDMEM 0.1% BSA. Cells were labeled with DiI fluorescent vital dye (MolecularProbes) for 20 minutes at 37°C and plating $1x10^5$ cells in the upper chamber of transwell-like inserts, carrying a fluorescence-shielding porous polyethylene terephthalate membrane with 8 µm pores (HTS Fluoroblok, BD) and then incubated at 37°C for the an overnight. The lower chamber was filled with serum free

medium supplemented with 5% WF plus PF-4708671 (10 μM) or Temsirolimus (100 nM), as indicated.

For evasion assay, $7.5x10^3$ cells were included in Matrigel (Cultrex, BME) drops at the final concentration of 6 mg/ml (12μl of matrix volume per drops). Matrigel was diluted in DMEM 0.1% BSA. The drops, sufficiently spaced from one another, were dispensed in cell culture dishes and maintained for 1 h at 37°C upside down to let jellify. Then, the dishes were turned up and the drops incubated in complete medium or serum free medium supplemented with 5% WF. The evasion ability was evaluated 6 days after inclusion by measuring the distance covered by crystal violet-stained cells exited from the drops (5 drops/cell lines/experiment). Images were collected using a stereo microscope Leica M205FA.

5.10. RNA extraction, RT-PCR and qRT-PCR

RNA from mouse samples (primary tumors and recurrences) or from cells was extracted using TRIzol (Invitrogen). Disruption of the tissue sample was achieved by grinding the frozen tissue using the TissueLyser II (Qiagen). Complete homogenization was achieved by passing the lysate at least 5 times through a 23-gauge needle fitted to an RNase-free syringe. RNA was then quantified and retro-transcribed with AMV Reverse Transcriptase (according to provider's instruction, Promega) to obtain cDNAs. The obtained cDNAs were amplified by PCR in order to confirm the presence in the recurrences of the same cell injected. The following primers designed on vectors were used:

pMSCV FW, 5'-CCCTTGAACCTCCTCGTTCGACC-3';

pMSCV RW, 5'GAGACGTGCTACTTCCATTTGTC-3'.

Absolute expression of human Bcl-2, Survivin and Cyclin D1 was evaluated by qRT-PCR using SYBR Green dye-containing reaction buffer (Experteam). The primers (SIGMA) used were:

human Bcl-2 FW, 5-TCCGATCAGGAAGGCTAGAGTT-3';

human Bcl-2 RW, 5'-CGGTCTCCTAAAAGCAGGC-3'

human Survivin FW: 5'-CCACCGCATCTCTACATTCA-3'

human Survivin RW: 5'-TATGTTCCTCTATGGGGTCG-3'

human Cyclin D1 FW: 5'-AGAAGGAGGTCCTGCCGTCC-3'

human Cyclin D1 RW: 5'-GGTCCAGGTAGTTCATGGCC-3'

Standard curves (10-fold dilution from 10^1 to 10^{-4} attomoles) were prepared both for target genes and for housekeeping genes. The incorporation of the SYBR Green dye into the PCR products was monitored in real time using the iQ5 Biorad real-time PCR detection system,

and the resulting threshold cycles (Ct) were computed. Ct values were converted into attomoles and the normalized target gene value was obtained by using at least two different housekeeping genes.

5.11. Apoptosis assays

To evaluate cell survival in adhesion-independent growth, cell attachment was prevented by coating Petri dishes with 12mg/ml Poly-HEMA in 95% ethanol (poly-2-hydroxyethyl methacrylate, SIGMA). MDA-MB-231 cells were plated in Poly-HEMA coated dishes in serum free medium and cultured for the indicated time points. Where indicated, PF-4708671 and Temsirolimus were added to the medium at the final concentration of 10 μM or 100 nM, respectively. Apoptosis was subsequently measured by TUNEL assay: $3x10^4$ cells were washed in PBS and cytospinned on a glass slide, (Shandon Cytospin 4, Thermo Scientific). Detection of apoptosis was performed using In Situ Cell Death Detection Kit, AP (Roche), according to the manufacturer's instructions. Apoptotic rate was calculated as the ratio of positive cells over the total number/field. Images were acquired using Leica fluorescence microscope (DMI6000B) equipped with a 20X objective.

5.12. Side population analysis

To identify side population, MCF-7 cells were resuspended in DMEM containing 2%FBS and 10mM HEPES at $1x10^6$ cells/ml in the presence or not of ABC transporter inhibitor, Reserpine (Sigma, 50μM) and were incubated for 5 minutes at 37°C. After, cells were incubated with Hoechst 33342 (Sigma, 5μg/ml) for 90 minutes at 37°C. After staining, the cells were washed in wash buffer (HBSS containing 2%FBS and 10mM HEPES) and were centrifuged for 7 minutes at 1200 rpm. Cells were resuspended in 200 μl of wash buffer and 7-AAD (2 μg/ml) was added for 10 minutes before FACS analysis, which allows the discrimination of dead versus live cells. Analyses sorting were done on a FACS LSRFortessa (Becton Dickinson). The Hoechst 33342 dye was excited at 357 nm and its fluorescence was dual-wavelength analyzed (blue, 402–446 nm; red, 650–670 nm).

5.13. Mammospheres Assay

To establish primary mammospheres, cells were plated in poly-HEMA coated dishes as single cell suspension (6000 cells in 35 mm dishes). Standard mammosphere medium contains phenol red-free DMEM/F12 (Gibco), B27 supplement (no vitamin A; Invitrogen) and recombinant epidermal growth factor (rEGF, 20 ng/ml; Sigma). Where indicated, cell were

plated in medium containing phenol red-free DMEM/F12, B27 supplement and 5% WF. In a subset of experiments, blocking antibody anti-IL6 (R&D Systems, 0.2μg/ml) or STAT3 inhibitors (STAT3 inhibitor VI S3I-201 50μM for MDA-MB-231, 100μM for MDA-MB-468; STA-21 30μM for both the cell lines; STAT3 inhibitor V Stattic 10μM for both the cell lines and Galiellalactone 12μM for MDA-MB-231, 25μM for MDA-MB-468) were added at the medium. After ten days, primary mammospheres were counted using a 4X objective. To establish secondary mammospheres, primary mammospheres were collected, resuspended in 0.5 % trypsin/0.2 % EDTA and disaggregate using 25-gauge needle fitted to a syringe. Cells were plated in the medium at the same seeding density that was used in the primary generation. Mammosphere forming efficiency (MFE%) was calculated as follows: number of mammospheres per well/number of cells seeded per well x 100. Mammosphere self-renewal was calculated as follows: total number of 2nd mammospheres formed/total number of 1st mammospheres formed. For more details see Ref 119.

5.14. Immunoassay for the detection of phosphorylation of STAT proteins

The detection of the activation of STAT phospho-protein was performed using the Milliplex Map 5-Plex Human STAT Phosphoprotein Magnetic Bead Kit. MDA-MB-231 cells were starved and stimulated or not with WF 5% for 20 minutes and processed as indicated by the manufacturer's instruction.

5.15. *In vivo* experiments

Primary tumors were established by injection of $2x10^6$ MDA-MB-231 control or derived cell clones bilaterally in the fat pads of the thoracic mammary glands of female athymic nude mice (Harlan, 6-8 weeks old). As indicated, a subset of experiments was performed inoculating MDA-MB-231 control cell ($2x10^6$ or $1x10^6$) in the left MFP and MDA-MB-231 p70KR cells or MDA-MB-231 sh-STAT3 ($2x10^6$) in the controlateral one. Growth of primary tumors was monitored by measuring tumor length (L) and width (W), and calculating tumor volume based on the formula $L \times W^2 / 2$. For the evaluation of local relapse, pre-anesthetized mice underwent breast surgery to remove the primary tumors, when tumors reached a volume of 200-300 mm^3. The appearance of locale recurrence was monitored by macroscopic examination of mice over a period of 8 weeks. Unless tumor burden was incompatible with the well-being of the animals, mice were sacrificed at the end of experiment. Recurrent disease or mammary glands, axillary/brachial lymph nodes and lungs were collected and stored together with the primary tumors for the subsequent analyses.

To evaluate the effect of PF-4708671 and Temsirolimus on the formation of recurrences, primary tumors were established by injection of $2x10^6$ MDA-MB-231 control cells, as described above. The animals were randomly divided into groups according to experimental design (5 mice/control group, 5 mice/treatment/concentration). The administration of the drugs was performed following a "peri-operative schedule". Mice were intraperitoneally injected with PF-4708671 (600 μg per mouse, equivalent to 25 mg/kg, or 1200 μg per mouse, equivalent to 50 mg/kg, diluted in PBS) or Temsirolimus (300 μg per mouse, equivalent to 12.5 mg/kg, or 600 μg per mouse,equivalent to 25 mg/kg, diluted in PBS) or vehicle (PBS) daily, for three days in succession. First treatment was on day -1, second on the day of surgery and third treatment on day +1.

In the long-term treatment experiment, after the appearance of palpable primary tumors generated from MDA-MB-231 control cells, animals were intraperitoneally treated with PF-4708671 (600 μg per mouse) or Temsirolimus (300 μg per mouse) twice a week, for three weeks. During treatment, growth of primary tumors was monitored and measured. Mice were sacrificed at the end point of the experiment. To evaluate the effect of the three-days schedule of treatment on tumor cells *in vivo*, primary tumors were established by injection of $2x10^6$ MDA-MB-231 control cells, bilaterally in thoracic MFP. When primary tumors reached a volume of 50-100 mm^3, mice were intraperitoneally treated with PF-4708671 (3 mice/group, 1200 μg/mouse) or with Temsirolimus (3 mice/group, 300 μg or 600 μg/mouse) or vehicle (3 mice/group, PBS) daily, for three consecutive days. Mice were sacrificed one day after the last treatment. Tumors were collected and stored for subsequent analyses. To analyze the tumor take rate, mice were injected with $1x10^4$ or $2x10^4$ or $5x10^4$ or $1x10^5$ or $2x10^5$ or $7.5x10^5$ or $2x10^6$ MDA-MB-231 control or modified cells resuspended in 50 μl Matrigel/PBS (1:1). Growth of primary tumors was monitored up to 8 weeks. As an alternative approach, mice were injected with $1x10^5$, $2x10^5$ or $4x10^5$ MDA-MB-231 control- or p70KR expressing-cells, without Matrigel, in 100μl of PBS. Growth of primary tumors was monitored up to 8 weeks.

5.16. Statistical analyses

Data were examined using the two-tailed Student t test or unpaired two-tailed Mann-Whitney U test. Differences were considered significant at $p < 0.05$. Significance in disease-free survival curve was calculated using Logrank test along with Hazard Ratio. The computer software PRISM (version 4, GraphPad, Inc.) was used to make graphs and all statistical analyses.

6. REFERENCES

1. Hortobagyi GN, de la Garza Salazar J, Pritchard K, et al. The global breast cancer burden: variations in epidemiology and survival. Clin Breast Cancer 2005; 6: 391-401.
2. Berry DA, Cronin KA, Plevritis SK, et al. Effect of screening and adjuvant therapy on mortality from breast cancer. N Engl J Med 2005; 353: 1784-1792.
3. Siegel R, Naishadham D, Jemal A. Cancer Statistics CA Cancer J Clin 2013; 63: 11-30.
4. Bosetti C, Bertuccio P, Malvezzi M, et al. Cancer mortality in Europe, 2005–2009, and an overview of trends since 1980. Ann Oncol 2013; 24: 2657-2671.
5. Higgins MJ, Baselga J. Targeted therapies for breast cancer. J Clin Invest 2011; 121: 3797-3803.
6. Perou CM, Sorlie T, Eisen MB, et al. Molecular portraits of human breast tumours. Nature 2000; 406: 747-752.
7. Sorlie T, Perou CM, Tibshirani R, et al. Gene expression patterns of breast carcinomas distinguish tumor subclasses with clinical implications. Proc Natl Acad Sci U S A 2001; 98: 10869-10874.
8. Prat A, Perou CM. Deconstructing the molecular portraits of breast cancer. Mol Oncol 2011; 5: 5-23.
9. Perou CM, Børresen-Dale AL. Systems Biology and Genomics of Breast Cancer. Cold Spring Harb Perspect Biol 2011; 1;3(2)
10. Mohamed A, Krajewski K, Cakar B, et al. Targeted Therapy for Breast. Am J Pathol 2013; 183: 1096-1112.
11. Benson JR, Jatoi I, Keisch M, et al. Early breast cancer. Lancet 2009; 373:1463-1479.
12. Komoike Y, Akiyama F, Iino Y, et al. Analysis of ipsilateral breast tumor recurrences after breast-conserving treatment based on the classification of true recurrences and new primary tumors. Breast Cancer 2005; 12:104-111.
13. Early Breast Cancer Trialists' Collaborative Group (EBCTCG).Clarke M, Collins R, Darby S, et al. Effects of radiotherapy and of differences in the extent of surgery for early breast cancer on local recurrence and 15 year survival: an overview of the randomised trials. Lancet 2005; 366: 2087–2106.
14. Brewster AM, Hortobagyi GN, Broglio KR,et al. Residual risk of breast cancer recurrence 5 years after adjuvant therapy. J Natl Cancer Inst 2008; 100: 1179–1183.
15. Fisher B, Anderson S, Fisher ER, et al. Significance of ipsilateral breast tumour recurrence after lumpectomy. Lancet 1991; 338: 327-31.
16. Veronesi U, Marubini E, Del Vecchio M, et al. Local recurrences and distant metastases after conservative breast cancer treatments: partly independent events. J Natl Cancer Inst 1995; 87: 19-27.
17. Whelan T, Clark R, Roberts R, et al. Ipsilateral breast tumor recurrence post-lumpectomy is predictive of subsequent mortality: results from a randomized trial. Int J Radiat Oncol Biol Phys 1994; 30:11-6.
18. Early Breast Cancer Trialists' Collaborative Group (EBCTCG). Darby S, McGale P, Correa C, et al. Effect of radiotherapy after breast-conserving surgery on 10-year recurrence and 15-year breast cancer death: meta analysis of individual patient data for 10,801 women in 17 randomised trials. Lancet 2011; 378:1707-1716.

19. Goss PE, Chambers AF. Does tumour dormancy offer a therapeutic target? Nat Rev Cancer 2010; 10:871–877.
20. Saphner T, Tormey DC, Gray R. Annual hazard rates of recurrence for breast cancer after primary therapy. J Clin Oncol 1996; 14:2738–2746.
21. Early Breast Cancer Trialists' Collaborative Group (EBCTCG). Clarke M, Collins R, Darby S, et al. Effects of chemotherapy and hormonal therapy for early breast cancer on recurrence and 15-year survival: an overview of the randomised trials. Lancet 2005; 365:1687–1717.
22. Voduc KD, Cheang MC, Tyldesley S, et al. Breast Cancer Subtypes and the Risk of Local and Regional Relapse. J Clin Oncol 2010; 28:1684-1691.
23. Dent R, Trudeau M, Pritchard KI, et al. Triple-negative breast cancer: clinical features and patterns of recurrence. Clin Cancer Res. 2007; 13:4429-4434.
24. Baker DG, Masterson TM, Pace R, et al. The influence of the surgical wound on local tumor recurrence. Surgery 1989; 106:525-32.
25. Demicheli R, Valagussa P, Bonadonna G, et al. Does surgery modify growth kinetics of breast cancer micrometastases? Br J Cancer 2001; 85:490-492.
26. Demicheli R, Retsky MW, Hrushesky WJ, et al. Tumor dormancy and surgery-driven interruption of dormancy in breast cancer: learning from failures. Nat Clin Pract Oncol 2007; 12:699-710.
27. Vaidya JS, Joseph DJ, Tobias JS, et al. Targeted intraoperative radiotherapy versus whole breast radiotherapy for breast cancer (TARGIT-A trial): an international, prospective, randomised, non-inferiority phase 3 trial. Lancet 2010; 376:91-102.
28. Veronesi U, Saccozzi R, Del Vecchio M, et al. Comparing radical mastectomy with quadrantectomy, axillary dissection, and radiotherapy in patients with small cancers of the breast. N Engl J Med 1981; 305:6–11.
29. Iozzo RV. Tumor stroma as a regulator of neoplastic behavior. Agonistic and antagonistic elements embedded in the same connective tissue. Lab Invest 1995; 73:157–160.
30. Ronnov-Jessen L, Petersen OW, Bissell MJ. Cellular changes involved in conversion of normal to malignant breast: importance of the stromal reaction. Physiol Rev 1996; 76:69-125.
31. Troester MA, Lee MH, Carter M, et al. Activation of Host Wound Responses in Breast Cancer microenvironment. Clin Cancer Res 2009; 15:7020-7028.
32. Fisher B, Gunduz N, Coyle J, et al. Presence of a growth-stimulating factor in serum following primary tumor removal in mice. Cancer Res 1989; 49:1996-2001.
33. Belletti B, Vaidya JS, D'Andrea S, et al. Targeted intraoperative radiotherapy impairs the stimulation of breast cancer cell proliferation and invasion caused by surgical wounding. Clin Cancer Res 2008; 14:1325-1332.
34. Tagliabue E, Agresti R, Carcangiu ML, et al. Role of HER2 in wound-induced breast carcinoma proliferation. Lancet 2003; 362: 527-533.
35. Vaidya JS, Wenz F, Bulsara M, et al. Risk-adapted targeted intraoperative radiotherapy versus whole-breast radiotherapy for breast cancer: 5-year results for local control and overall survival from the TARGIT-A randomised trial. Lancet 2013; in press

36. Ghayad SE, Cohen PA. Inhibitors of the PI3K/Akt/mTOR pathway: new hope for breast cancer patients. Recent Pat Anticancer Drug Discov 2010; 5:29-57.
37. Pearce LR, Komander D, Alessi DR, et al. The nuts and the bolts of AGC protein kinases. Nat Rev Mol Cell Biol 2010; 11:9-22.
38. Fingar DC, Blenis J. Target of rapamycin (TOR): an integrator of nutrient and growth factor signals and coordinator of cell growth and cell cycle progression. Oncogene 2004; 23:3151-3171.
39. Kim D, Dan HC, Park S, et al. AKT/PKB signaling mechanisms in cancer and chemoresistance. Front Biosci 2005; 10: 975-987.
40. Hennessy BT, Smith DL, Ram PT, et al. Exploiting the PI3K/AKT pathway for cancer drug discovery. Nat Rev Drug Discov 2005; 4:988-1004.
41. Altomare DA, Testa JR. Perturbations of the AKT signaling pathway in human cancer. Oncogene 2005; 24:7455-7464.
42. Hay N, Sonenberg N. Upstream and downstream of mTOR. Genes Dev 2004; 18: 1926–1945.
43. Efeyan A, Sabatini DM. mTOR and cancer: Many loops in one pathway. Curr Opin Cell Biol 2010; 22:169-176.
44. Guertin DA, Sabatini DM.Defining the role of mTOR in cancer. Cancer Cell 2007; 12:9-22.
45. Pause A, Belsham GJ, Gingras AC, et al. Insulin-dependent stimulation of protein synthesis by phosphorylation of a regulator of 5'-cap function. Nature 1994; 371:762-767.
46. von Manteuffel SR, Dennis PB, Pullen N, et al. The insulin-induced signaling pathway leading to S6 and initiation factor 4E binding protein 1 phosphorylation bifurcates at a rapamycin-sensitive point immediately upstream of p70S6K. Mol Cell Biol 1997; 17:5426-5436.
47. Fenton TR, Gout IT. Functions and regulation of the 70kDa ribosomal S6 kinase. Int J Biochem Cell Biol. 2011; 43:47-59.
48. Ma XM, Blenis J. Molecular mechanisms of mTOR-mediated translational control. Nat Rev Mol Cell Biol 2009; 10:307–318.
49. Düvel K, Yecies JL, Menon S, et al. Activation of a metabolic gene regulatory network downstream of mTOR complex 1. Mol Cell 2010; 39:171-183.
50. Shin S, Wolgamott L, Yu Y, et al. Glycogen synthase kinase (GSK)-3 promotes p70 ribosomal protein S6 kinase (p70S6K) activity and cell proliferation. Proc Natl Acad Sci U S A 2011; 108:E1204-1213.
51. Kawasome H, Papst P, Webb S, et al. Targeted disruption of p70(s6k) defines its role in protein synthesis and rapamycin sensitivity. Proc Natl Acad Sci U S A 1998; 95:5033-5038.
52. Hershey JW, Sonenberg N, Mathews MB, et al. Principles of translational control: an overview. Cold Spring Harbor Perspec Biol 2012; 1;4(12).
53. Bandi HR, Ferrari S, Krieg J, et al. Identification of 40 S ribosomal protein S6 phosphorylation sites in Swiss mouse 3T3 fibroblasts stimulated with serum. J Biol Chem 1993; 268:4530–4533.

54. Ferrari S, Bandi HR, Hofsteenge J, et al. Mitogen-activated 70K S6 kinase. Identification of in vitro 40 S ribosomal S6 phosphorylation sites. J Biol Chem 1991; 266:22770–22775.
55. Montagne J, Stewart MJ, Stocker H, et al. Drosophila S6 kinase: a regulator of cell size. Science 1999; 285:2126–2129.
56. Shima H, Pende M, Chen Y, et al. Disruption of the p70(s6k)/p85(s6k) gene reveals a small mouse phenotype and a new functional S6 kinase. Embo J 1998; 17:6649–6659.
57. Pende M,Um SH, Mieulet V, et al. S6K1(−/−)/S6K2(−/−) mice exhibit perinatal lethality and rapamycin-sensitive 5-terminal oligopyrimidine mRNA translation and reveal a mitogen-activated protein kinase dependent S6 kinase pathway. Mol Cell Biol 2004; 24:3112–3124.
58. Wang X, Li W, Williams M, et al. Regulation of elongation factor 2 kinase by p90(RSK1) and p70 S6 kinase. Embo J 2001; 20:4370–4379.
59. Raught B, Peiretti F, Gingras AC, et al. Phosphorylation of eucaryotic translation initiation factor 4B Ser422 is modulated by S6 kinases. Embo J 2004; 23:1761–1769.
60. Dorrello NV, Peschiaroli A, Guardavaccaro D, et al. S6K1- and beta TRCP-mediated degradation of PDCD4 promotes protein translation and cell growth. Science 2006; 314:467–471.
61. Richardson CJ, Broenstrup M, Fingar DC, et al. SKAR is a specific target of S6 kinase 1 in cell growth control. Curr Biol 2004; 14:1540–1549.
62. Holz MK, Ballif BA, Gygi SP, et al. mTOR and S6K1 mediate assembly of the translation preinitiation complex through dynamic protein interchange and ordered phosphorylation events. Cell 2005; 123:569–580.
63. Skinner HD, Zheng JZ, Fang J, et al. Vascular endothelial growth factor transcriptional activation is mediated by hypoxia-inducible factor 1alpha, HDM2, and p70S6K1 in response to phosphatidylinositol 3-kinase/AKT signaling. J Biol Chem 2004; 279:45643-45651.
64. Zhou HY, Wong AS.Activation of p70S6K induces expression of matrix metalloproteinase 9 associated with hepatocyte growth factor-mediated invasion in human ovarian cancer cells. Endocrinology 2006; 147:2557–2566.
65. Couch FJ, Wang XY, Wu GJ, et al. Localization of PS6K to chromosomal region 17q23 and determination of its amplification in breast cancer. Cancer Res 1999; 59:1408-1411.
66. Monni O, Barlund M, Mousses S, et al. Comprehensive copy number and gene expression profiling of the 17q23 amplicon in human breast cancer. Proc Natl Acad Sci US A 2001; 98:5711-5716.
67. Barlund M, Forozan F, Kononen J, et al. Detecting activation of ribosomal protein S6 kinase by complementary DNA and tissue microarray analysis. J Natl Cancer Inst 2000; 92:1252-1259.
68. Sinclair CS, Rowley M, Naderi A, et al. The 17q23 amplicon and breast cancer. Breast Cancer Res Treat 2003; 78:313-322.
69. Lin HJ, Hsieh FC, Song H, et al. Elevated phosphorylation and activation of PDK-1/AKT pathway in human breast cancer. Br J Cancer 2005; 93:1372-1381.

70. van der Hage JA, van den Broek LJ, Legrand C, et al. Overexpression of P70 S6 kinase protein is associated with increased risk of locoregional recurrence in node-negative premenopausal early breast cancer patients. Br J Cancer. 2004; 90:1543-1550.
71. Sabatini DM. mTOR and cancer: insights into a complex relationship. Nat Rev Cancer 2006; 6:729-734.
72. Guertin DA, Sabatini DM. An expanding role for mTOR in cancer. Trends Mol Med 2005; 11:353–361.
73. Teachey DT, Obzut DA, Cooperman J, et al. The mTOR inhibitor CCI-779 induces apoptosis and inhibits growth in preclinical models of primary adult human ALL. Blood 2006; 107:1149–1155.
74. Thimmaiah KN, Easton J, Huang S, et al. Insulin-like growth factor Imediated protection from rapamycin-induced apoptosis is independent of Ras-Erk1-Erk2 and phosphatidylinositol 3-kinase–Akt signaling pathways. Cancer Res 2003; 63:364-374.
75. Sun SY, Rosenberg LM, Wang X, et al. Activation of Akt and eIF4E survival pathways by rapamycin-mediated mammalian target of rapamycin inhibition. Cancer Res. 2005; 65: 7052-7058.
76. O'Reilly KE, Rojo F, She QB, et al. mTOR inhibition induces upstream receptor tyrosine kinase signaling and activates Akt. Cancer Res. 2006; 66:1500-1508.
77. Mantovani A, Allavena P, Sica A, et al.Cancer-related inflammation. Nature 2008; 454:436–444.
78. Yu H, Pardoll D, Jove R. STATs in cancer inflammation and immunity: a leading role for STAT3. Nat Rev Cancer 2009; 9:798-809.
79. Calò V, Migliavacca M, Bazan V et al. STAT Proteins: From Normal Control of Cellular Events to Tumorigenesis. J Cell Physiol 2003; 197: 157-168.
80. Schindler C, Darnell JE Jr. Transcriptional responses to polypeptide ligands: the JAK-STAT pathway. Annu Rev Biochem 1995; 64:621–651.
81. Darnell JE Jr. STATs and gene regulation. Science 1997; 277:1630–1635.
82. Horvath CM. STAT proteins and transcriptional responses to extracellular signals. Trends Biochem Sci 2000; 25:496–502.
83. Grandis JR, Drenning SD, Chakraborty A, et al. Requirement of Stat3 but not Stat1 activation for epidermal growth factor receptor mediated cell growth in vitro. J Clin Invest 1998; 102:1385–1392.
84. Trevino JG, Gray MJ, Nawrocki ST, et al. Src activation of Stat3 is an independent requirement from NF-κB activation for constitutive IL-8 expression in human pancreatic adenocarcinoma cells. Angiogenesis 2006; 9:101-110.
85. Zhong Z, Wen Z, Darnell JE Jr. Stat3: a STAT family member activated by tyrosine phosphorylation in response to epidermal growth factor and interleukin-6. Science 1994; 264: 95–98.
86. Darnell JE Jr, Kerr IM, Stark GR. Jak-STAT pathways and transcriptional activation in response to IFNs and other extracellular signaling proteins. Science 1994; 264:1415–1421.
87. Schindler C, Levy DE, Decker T. JAK-STAT signaling: from interferons to cytokines. J Biol Chem 2007; 282:20059–20063.

88. Levy DE, Darnell JE Jr. Stats: transcriptional control and biological impact. Nat Rev Mol Cell Biol 2002; 3:651–662.
89. Heinrich PC, Behrmann I, Muller-Newen G, et al. Interleukin-6-type cytokine signalling through the gp130/Jak/STAT pathway. Biochem J 1998; 334:297–314.
90. Yu H, Kortylewski M, Pardoll D. Crosstalk between cancer and immune cells role of STAT3 in the tumour microenvironment. Nat Rev Immunol 2007; 7:41–51.
91. Al Zaid Siddiquee K, Turkson J. STAT3 as a target for inducing apoptosis in solid and hematological tumors. Cell Res 2008;18: 254–67.
92. Bowman T, Garcia R, Turkson J, et al. STATs in oncogenesis. Oncogene 2000;19:2474-2488.
93. Turkson J, Bowman T, Garcia R, et al. Stat3 activation by Src induces specific gene regulation and is required for cell transformation. Mol Cell Biol 1998;18:2545-2552.
94. Bromberg JF, Horvath CM, Besser D, et al. Stat3 activation is required for cellular transformation by v-src. Mol Cell Biol 1998; 18:2553-2558.
95. Schlessinger K, Levy DE. Malignant transformation but not normal cell growth depends on signal transducer and activator of transcription 3. Cancer Res 2005;65:5828-5834.
96. Bromberg JF, Wrzeszczynska MH, Devgan G, et al. Stat3 as an oncogene. Cell 1999; 98:295-303.
97. Furth PA. STAT signaling in different breast cancer sub-types. Mol Cell Endocrinol 2014; 382: 612-615.
98. Garcia R, Bowman TL, Niu G, et al. Constitutive activation of Stat3 by the Src and JAK tyrosine kinases participates in growth regulation of human breast carcinoma cells. Oncogene 2001; 20:2499-2513.
99. Garcia R, Yu CL, Hudnall A, et al. Constitutive activation of Stat3 in fibroblasts transformed by diverse oncoproteins and in breast carcinoma cells. Cell Growth Differ 1997; 8:1267-1276.
100. Diaz N, Minton S, Cox C, et al. Activation of stat3 in primary tumors from high-risk breast cancer patients is associated with elevated levels of activated SRC and survivin expression. Clin Cancer Res 2006; 12:20-28.
101. Berishaj M, Gao SP, Ahmed S, et al. Stat3 is tyrosine-phosphorylated through the interleukin-6/glycoprotein 130/Janus kinase pathway in breast cancer. Breast Cancer Res 2007; 9:R32.
102. Berclaz G, Alternatt HJ, Rohrbach V, et al. EGFR dependent expression of Stat3 (but not Stat1) in breast cancer. Int J Oncol 2001; 19:1155–1160.
103. Dolled-Filhart M, Camp RL, Kowalski DP, et al. Tissue microarray analysis of signal transducers and activators of transcription3 (Stat3) and phospho-Stat3 in node-negative breast cancer shows nuclear localization is associated with a better prognosis. Clin Cancer Res 2003; 9:594–600.
104. Siddiquee K, Zhang S, Guida WC, et al. Selective chemical probe inhibitor of Stat3, identified through structure-based virtual screening, induces antitumor activity. Proc Natl Acad Sci U S A 2007;104:7391–7396.

105. Real PJ, Sierra A, De Juan A, et al. Resistance to chemotherapy via Stat3-dependent overexpression of Bcl-2 in metastatic breast cancer cells. Oncogene 2002; 21:7611–7618.
106. Liu S, Wicha MS. Targeting breast cancer stem cells. J Clin Oncol 2010; 28:4006-4012.
107. Korkaya H, Liu S, Wicha MS. Breast cancer stem cells, cytokine networks, and the tumor microenvironment. J Clin Invest 2011; 121:3804–3809.
108. Chaffer CL, Weinberg RA. A perspective on cancer cell metastasis. Science 2011; 331:1559–1564.
109. Li X, Lewis MT, Huang J, et al.Intrinsic resistance of tumorigenic breast cancer cells to chemotherapy. J Natl Cancer Inst 2008; 100:672–679.
110. Marotta LL, Almendro V, Marusyk A, et al. The JAK2/STAT3 signaling pathway is required for growth of CD44(+)CD24(−) stem cell-like breast cancer cells in human tumors. J Clin Invest 2011; 121:2723–2735.
111. Hernandez-Vargas H, Ouzounova M, Le Calvez-Kelm F, et al. Methylome analysis reveals Jak-STAT pathway deregulation in putative breast cancer stem cells. Epigenetics 2011; 6:428–439.
112. Dave B, Landis MD, Tweardy DJ, et al. Selective small molecule Stat3 inhibitor reduces breast cancer tumor-initiating cells and improves recurrence free survival in a human-xenograft model. Plos One 2012; 7:e30207.
113. Wolf J, Dewi DL, Fredebohm J, et al. A mammosphere formation RNAi screen reveals that ATG4A promotes a breast cancer stem-like phenotype. Breast Cancer Res 2013; 15:R109.
114. Turkson J. STAT proteins as novel targets for cancer drug discovery. Expert Opin Ther Targets 2004; 8:409-422.
115. Yu H, Jove R. The STATs of cancer: new molecular targets come of age. Nat Rev Cancer 2004; 4:97-105.
116. Yue P, Turkson J. Targeting STAT3 in cancer: how successful are we? Expert Opin Investig Drugs 2009; 18:45-56.
117. Schalm SS, Blenis J. Identification of a conserved motif required for mTOR signaling. Curr Biol. 2002; 12: 632-639.
118. Pearce LR, Alton GR, Richter DT, et al. Characterization of PF-4708671, a novel and highly specific inhibitor of p70 ribosomal S6 kinase (S6K1). Biochem J. 2010; 431:245-255.
119. Shaw FL, Harrison H, Spence K, et al. A detailed mammosphere assay protocol for the quantification of breast stem cell activity. J Mammary Gland Biol Neoplasia 2012; 17:111-117.
120. Tsuchida Y, Sawada S, Yoshioka I, et al. Increased surgical stress promotes tumor metastasis. Surgery 2003;133:547-555.
121. Bissell MJ, Hines WC. Why don't we get more cancer? A proposed role of the microenvironment in restraining cancer progression. Nat Med 2011; 17: 320-329.
122. Akar U, Ozpolat B, Mehta K, et al. Targeting p70S6K prevented lung metastasis in a breast cancer xenograft model. Mol Cancer Ther 2010; 9:1180-1187.

123. Harrington LS, Findlay GM, Gray A, et al. The TSC1-2 tumor suppressor controls insulin-PI3K signaling via regulation of IRS proteins. J Cell Biol 2004; 166:213–223.
124. Um SH, Frigerio F, Watanabe M, et al. Absence of S6K1 protects against age- and diet-induced obesity while enhancing insulin sensitivity. Nature 2004; 431:200-205.
125. Dar AC, Das TK, Shokat KM, et al. Chemical genetic discovery of targets and anti-targets for cancer polypharmacology. Nature 2012; 486:80-84.
126. Hsieh AC, Liu Y, Edlind MP, et al. The translational landscape of mTOR signaling steers cancer initiation and metastasis. Nature 2012; 485:55-61.
127. Carter CL, Allen C, Henson DE. Relation of tumor size, lymph node status, and survival in 24,740 breast cancer cases. Cancer 1989; 63: 181-187.
128. Sirohi B, Leary A, Johnston SR. Ipsilateral breast tumor recurrence: is there any evidence for benefit of further systemic therapy? Breast J 2009; 15:268-278.
129. Iliopoulos D, Hirsch HA, Struhl K. An Epigenetic Switch Involving NF-kB, Lin28, Let-7 MicroRNA, and IL6 Links Inflammation to Cell Transformation. Cell 2009; 139:693-706.
130. Lin SH, George TJ, Ben-Josef E, et al. Opportunities and Challenges in the Era of Molecularly Targeted Agents and Radiation Therapy. J Natl Cancer Inst 2013; 105:686-693.
131. Neve RM, Chin K, Fridlyand J, et al. A collection of breast cancer cell lines for the study of functionally distinct cancer subtypes. Cancer Cell 2006; 10: 515-527.

PUBLICATIONS

Mol Oncol, *in press* doi: 10.1016/j.molonc.2014.02.006
p70S6 Kinase Mediates Breast Cancer Cell Survival in Response to Surgical Wound Fluid Stimulation.
Ilenia Segatto, Stefania Berton, Maura Sonego, Samuele Massarut, Linda Fabris, Joshua Armenia, Alfonso Colombatti, Andrea Vecchione, Gustavo Baldassarre, Barbara Belletti.

Oncotarget, *advance on line publications*
Contact inhibition modulates intracellular levels of miR-223 in a p27kip1-dependent manner.
Joshua Armenia, Linda Fabris, Francesca Lovat, Stefania Berton, **Ilenia Segatto**, Sara D'Andrea, Ivan Cristina, Luciano Cascione, George A.Calin, Carlo M.Croce, Alfonso Colombatti, Andrea Vecchione, Barbara Belletti and Gustavo Baldassarre.

J Mol Cell Biol. 2013 Dec;5(6):428-31. doi: 10.1093/jmcb/mjt027. Epub 2013 Jul 29.
Inhibition of breast cancer local relapse by targeting p70S6 kinase activity.
Segatto I, Berton S, Sonego M, Massarut S, D'Andrea S, Perin T, Fabris L, Armenia J, Rampioni G, Lovisa S, Schiappacassi M, Colombatti A, Bristow RG, Vecchione A, Baldassarre G, Belletti B.

PLoS One. 2012;7(9):e45561. doi: 10.1371/journal.pone.0045561. Epub 2012 Sep 20.
Stathmin is dispensable for tumor onset in mice.
D'Andrea S, Berton S, **Segatto I**, Fabris L, Canzonieri V, Colombatti A, Vecchione A, Belletti B, Baldassarre G.

ACKNOWLEDGMENTS

This work was performed in the Division of Experimental Oncology 2 at the National Cancer Institute of Aviano, directed by Prof. Alfonso Colombatti.

I am grateful to all the members of the S.C.I.C.C. group, in particular I thank Dr. Barbara Belletti and Dr. Gustavo Baldassarre for their help and support.